A STUDY OF THE LOW-PASS CHARACTERISTICS OF LOADED RC DISTRIBUTED NETWORKS

A Thesis

Presented to

The Faculty of the Graduate Division

by

William F. Speights, Jr.

In Partial Fulfillment

of the Requirements for the Degree

Master of Science in Electrical Engineering

Georgia Institute of Technology

June, 1966

A STUDY OF THE LOW-PASS CHARACTERISTICS

OF LOADED RC DISTRIBUTED NETWORKS

Approved:

Chairman

Date approved by Chairman: 5-20-66

ACKNOWLEDGMENTS

The author would like to express his sincere appreciation to his thesis advisor, Dr. K. L. Su for his assistance and encouragement during the course of this investigation. He would also wish to thank the staff of the Rich Electronic Computer Center and the members of his reading committee, Dr. D. C. Fielder and Mr. C. R. Swenson, for their interest and constructive criticisms. A special note of appreciation is due Miss Elizabeth Irvine for her invaluable assistance in the preparation of the multitude of graphs included in this paper.

The author would also like to acknowledge the National Aeronautics and Space Administration for their support of this investigation.

TABLE OF CONTENTS

LIST OF ILLUSTRATIONS

LIST OF ILLUSTRATIONS (Continued)

LIST OF ILLUSTRATIONS (Continued)

LIST OF ILLUSTRATIONS (Continuted)

LIST OF TABLES

SUMMARY

The objective of this proposed research is to investigate the effects of terminating impedances on the voltage-transfer characteristics of RC distributed networks. Four general shapes of these networks are included in the investigation. The terminating impedances are limited to parallel combinations of a resistance and a capacitance. Previous studies of the open-circuit performance of networks from these four general shapes provide a basis for continued investigations of their loaded characteristics. The results of such investigations are presented throughout this paper. Through a comparison of these results it is possible to determine the value of proper shaping of RC thin-film networks that are terminated in parallel resistance-capacitance loads.

CHAPTER I

INTRODUCTION AND HISTORY

The recent trend in electronics toward compactness has stimulated abundant research in the field of miniaturization of both active and passive components. One solution to the problem of reducing the size of resistive and capacitive elements is the use of thin-film distributed networks. Because of their light weight, compactness, and rugged construction, these networks show promise of replacing conventional pig-tailed components in many engineering applications.

The simplest RC thin-film networks are made by depositing thin films of conductive, dielectric, and resistive materials in layers on supporting substrates as shown in Figure 1. Because of this sandwiching construction, the resistance and capacitance are distributed throughout the circuit with interacting fields, resulting in passive RC circuits with network functions that are unobtainable using lumped elements.

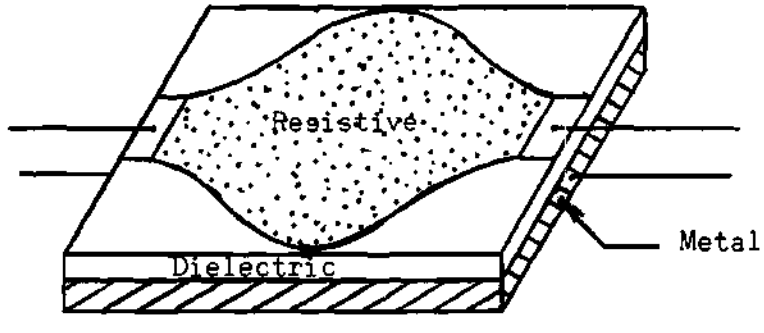

Figure 1. Composition of a Typical Thin-Film Network.

By varying the thickness and shape of the resistive and dielectric films and the location of connecting tabs, networks with various characteristics can be obtained.

As would be expected, mathematical analysis of distributed networks is much more complex than that of lumped-element networks. When the incremental resistance and capacitance are functions only of the displacement along the length of an RC distributed network, the network is essentially an RC transmission line. Therefore, for this type of network, methods of analysis have paralled transmission line theory.

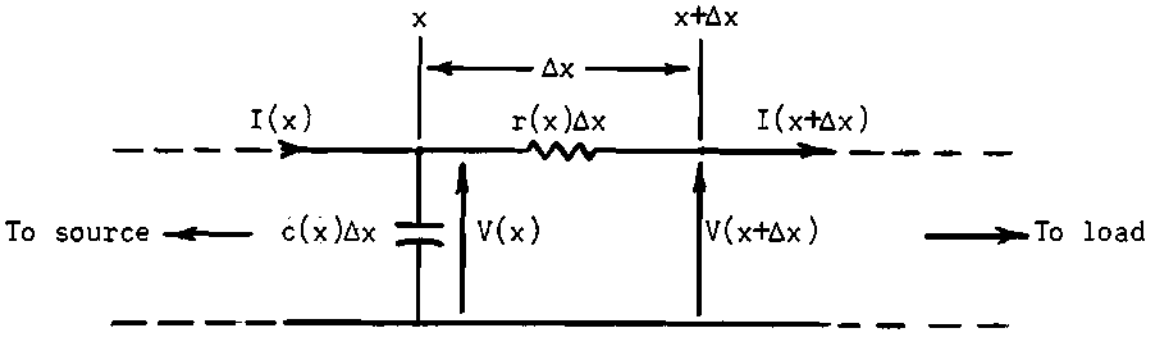

Figure 2. General RC Transmission Line.

Figure 2 shows an elementary length of a general RC transmission line. The differential equation that governs the behavior of such a line is

$$\frac{d^2V}{dx^2} - \frac{r'(x)}{r(x)}\frac{dV}{dx} - sr(x)c(x)V = 0 \qquad (1)$$

where V represents the complex amplitude of the voltage along the line, r(x) and c(x) are functions representing the variation of the resistance

and capacitance along the line, and s is the complex frequency variable.

Some effort has been expended by applied mathematicians in solving this equation in closed form.(16). It has been shown that such solutions are possible only when r(x) and c(x) are certain special, and usually complicated, functions.

If analysis is limited to the special case of RC lines for which the product of r(x) and c(x) is constant along the length of the line, equation (1) can be simplified considerably. It can be seen that for this restriction, the third coefficient of (1), the coefficient of V, is invariant with respect to x. Also, when such networks are fabricated in thin-film form, as shown in Figure 1, by depositing dielectric and resistive layers of uniform thickness on a metallic surface, the shaping of the resistance film such that r(x) varies in a prescribed way automatically produces the desired variation of c(x).

There are four general shapes of RC thin-film networks that have been analyzed up to date. It is convenient to classify these networks in accordance with the resistance variation along their length.

1. The resistance r(x) remains constant. This line is known as the uniform line. (3),(8)
2. The resistance r(x) either decreases or increases monotonically with x. The linear, (1),(9) the exponential (2),(6),(9),(17) and the Bessel (15) lines fall in this category.
3. The resistance r(x) first decreases and then increases with x. The trigonometric line (11) is one of this type.
4. The resistance r(x) first increases and then decreases with x. The hyperbolic line (12) is one in this category.

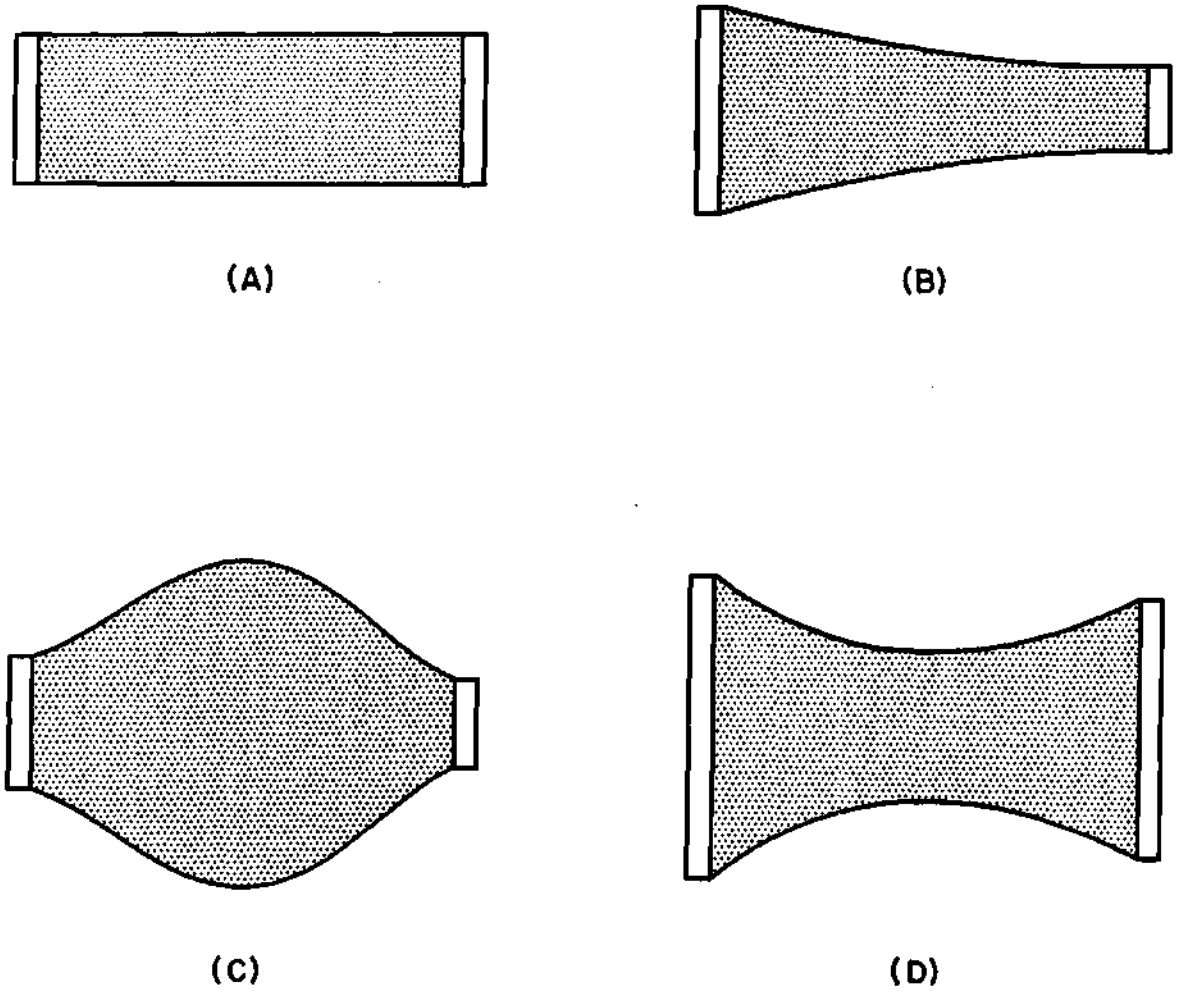

Figure 3. General Physical Shapes of RC-Thin-Film Networks

The general physical shape of each of these lines is illustrated in Figure 3.

So far, investigations of these thin-film networks have been limited to studies of their open-circuit performance. It has been shown that when the above networks are connected as illustrated in Figure 4, they all exhibit low pass open-circuit characteristics.

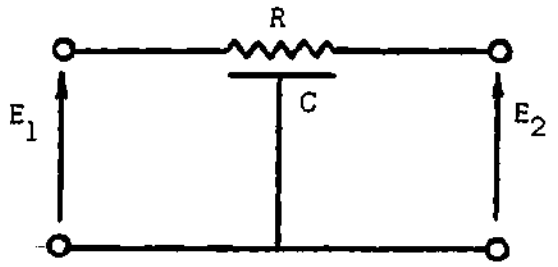

Figure 4. Schematic Symbol for an RC-Thin-Film Network.

Through comparisons of these low-pass characteristics, the advantages of proper shaping on the rate of attenuation have been demonstrated. For example, Kaufman and Garrett (9) showed that the cut-off rate for a network is generally improved as the ratio of $r(x_2)$ to $r(x_1)$, where x_2 and x_1 are the values of x at the output and input ports respectively, is increased. It should be noted that a line that is tapered for a higher cut-off rate will display a higer output impedance — high r and low c at the output port. Because of this high output impedance, it was suspected that the performance of such a network terminated at its output port would be quite different from that predicted for open-circuit conditions. Almost all investigations thus far have ignored this problem and confined themselves to the no-load

situation. It is the aim of this research to supplement these investigations with a study of the characteristics of thin-film networks terminated in load impedances.

When thin-film networks are used in conjunction with other passive and active components in fabricating electronic devices, the most common terminations can be represented as parallel combinations of a resistance and a capacitance. The Miller Effect model for the input circuit of certain transistor configurations is a typical example of the load impedance encountered by thin-film networks serving as coupling devices. It has therefore been decided to concentrate this study on the effects of a parallel resistance-capacitance termination, and the main objective of the research is to determine the value of proper shaping of RC thin-film networks under these terminated conditions.

Since a continued study of all the variously shaped networks listed on page 3 would, in many ways, be repetitive, it was decided to limit this investigation to one network from each of the four general shapes. These four networks are listed below along with corresponding descriptive equations which determine the variations in their incremental values of resistance and capacitance. Each pair of these equations appears in the following form:

$$r(x) = r_o f(x) \tag{2}$$

$$c(x) = c_o / f(x) \tag{3}$$

where x is the value of displacement in the direction of the length of the line with respect to the origin of its descriptive coordinate system,

and r_o and c_o are constants determined by the width thickness, and material composition of the network.

1. Uniform Line — $r(x) = r_o$ and $c(x) = c_o$; port 1 at $x = 0$, and port 2 at $x = \lambda$.
2. Exponential Line — $r(x) = r_o\varepsilon^{\alpha x}$ and $c(x) = c_o\varepsilon^{-\alpha x}$; port 1 at $x = 0$, and port 2 at $x = \lambda$.
3. Trigonometric Line — $r(x) = r_o \csc^2(x)$ and $c(x) = c_o \sin^2(x)$; port 1 at $x = x_1$, port 2 at $x = x_2$.
4. Hyperbolic Line — $r(x) = r_o \operatorname{sech}^2(x)$ and $c(x) = c_o \cosh^2(x)$; port 1 at $x = x_1$, and port 2 at $x = x_2$.

Figure 5 illustrates the location of each network within its respective coordinate system.

Even though the research is limited to these four specific lines, by choosing various values of x for the input and output ports, an unlimited number of actual networks are available. For example, an infinite number of hyperbolically tapered lines can be obtained by dividing the general hyperbolic line shown in Figure 5(D) into sections. Several results of this sectioning are shown in Figure 6. It is quite obvious that even though these are all hyperbolically tapered lines, their characteristics will differ quite noticeably.

Recent studies of the open-circuit characteristics of distributed networks provide a basis for a continued investigation of their loaded characteristics. Equations for the open-circuit impedance parameters of

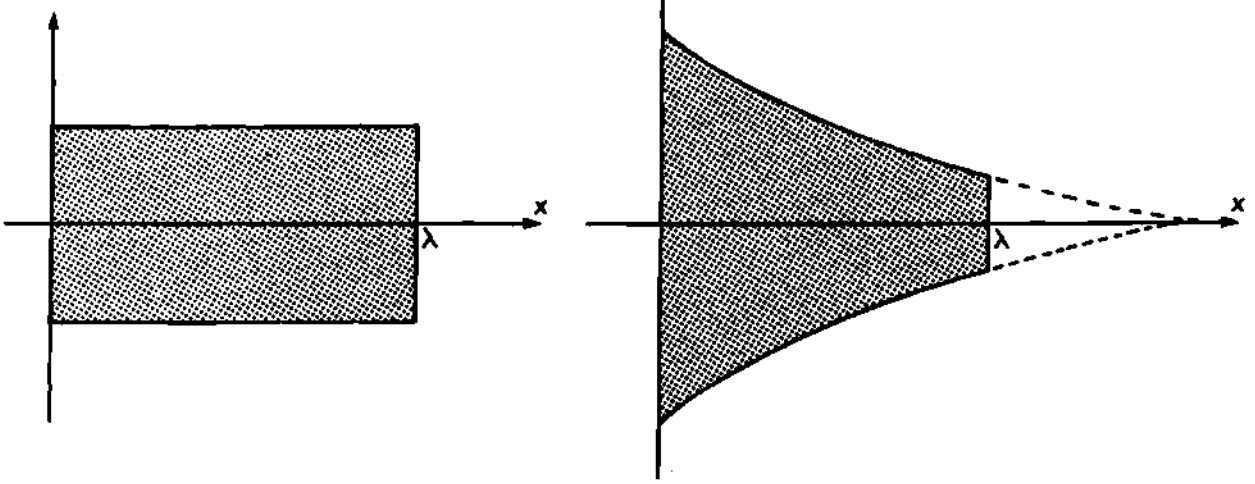

UNIFORM

(A)

EXPONENTIAL

(B)

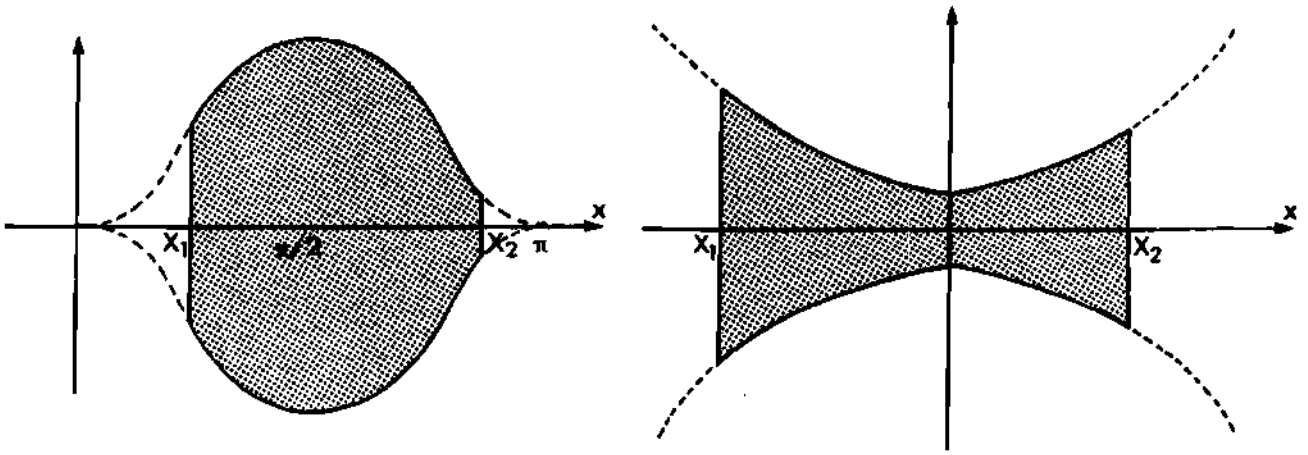

TRIGONOMETRIC

(C)

HYPERBOLIC

(D)

Figure 5. Descriptive Coordinate Systems for Four Specific Types of Thin-Film Networks

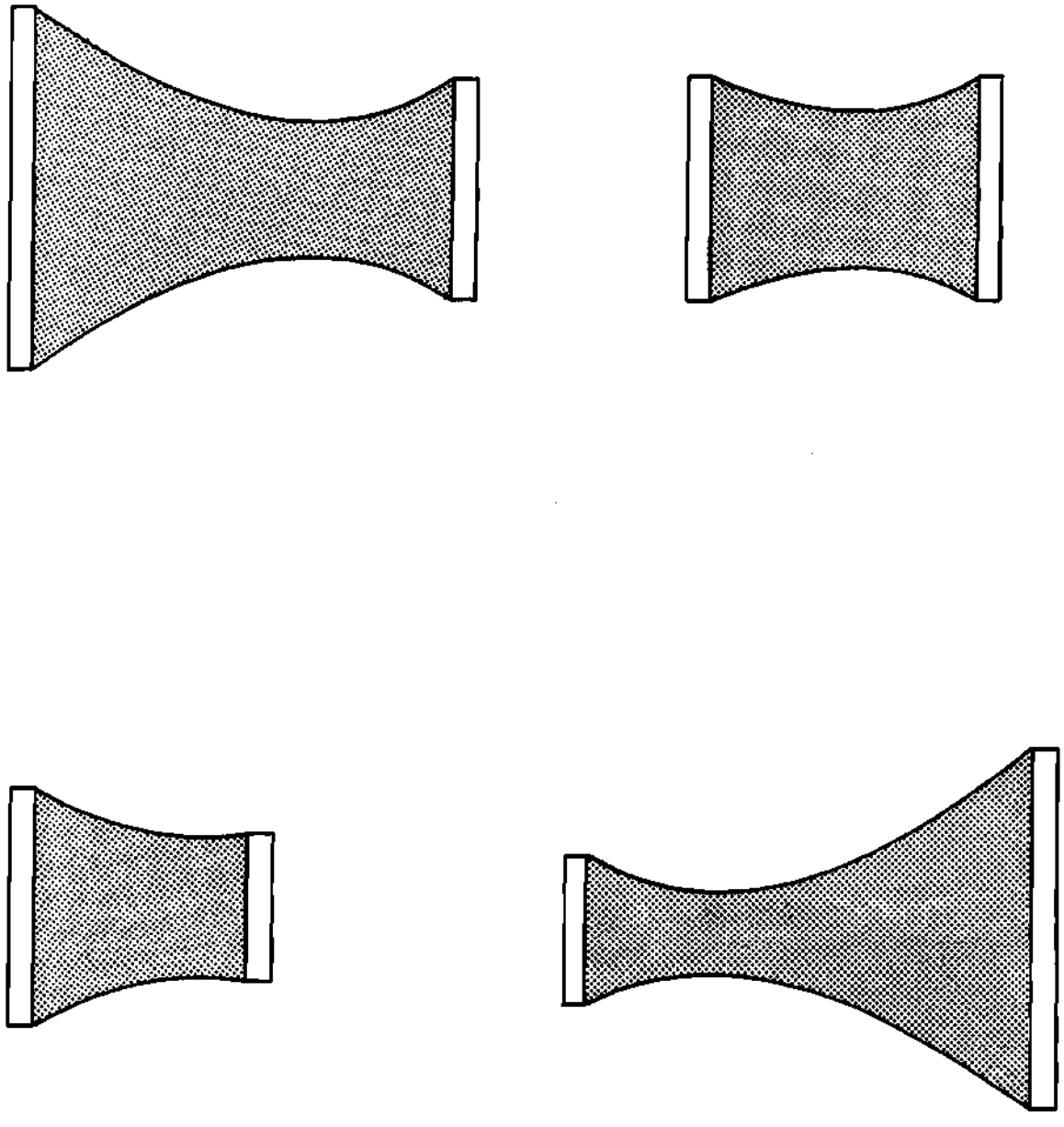

Figure 6. Variously Shaped Hyperbolic Lines

the four networks chosen for this study have been developed in several classical papers and are listed below for reference.

(1) The uniform line: (3)

$$z_{11} = z_{22} = \frac{r_o \lambda}{\theta \tanh \theta} \tag{4}$$

$$z_{12} = z_{21} = \frac{r_o \lambda}{\theta \sinh \theta} \tag{5}$$

where $\theta = \sqrt{s r_o c_o \lambda^2}$.

(2) The exponential line: (9)

$$z_{11} = \frac{1}{s c_o \lambda} \left[\frac{\theta}{\tanh \theta} + \frac{\alpha \lambda}{2} \right] \tag{6}$$

$$z_{12} = z_{21} = \frac{1}{s c_o \lambda} \frac{\theta \varepsilon^{\alpha \lambda / 2}}{\sinh \theta} \tag{7}$$

$$z_{22} = \frac{\varepsilon^{\alpha \lambda}}{s c_o \lambda} \left[\frac{\theta}{\tanh \theta} - \frac{\alpha \lambda}{2} \right] \tag{8}$$

where $\theta = \sqrt{\frac{\alpha^2 \lambda^2}{4} + s r_o c_o \lambda^2}$.

For $\alpha = 0$, the exponential line becomes a uniform line.

(3) The trigonometric line: (11)

$$z_{11} = \frac{r_o}{\Delta} \frac{\cos x_2 \sin b(x_2-x_1) - b \sin x_2 \cos b(x_2-x_1)}{\sin x_1} \tag{9}$$

$$z_{12} = z_{21} = -\frac{br_o}{\Delta} \tag{10}$$

$$z_{22} = \frac{r_o}{\Delta} \frac{\cos x_1 \sin b(x_2-x_1) + b \sin x_1 \cos b(x_2-x_1)}{\sin x_2} \tag{11}$$

where $b = \sqrt{1 - sr_oc_o}$ and

$$\Delta = \cos(x_2-x_1) \sin b(x_2-x_1) - b \sin(x_2-x_1) \cos b(x_2-x_1) - sr_oc_o \sin x_1 \sin x_2 \sin b(x_2-x_1).$$

(4) The hyperbolic line: (12)

$$z_{11} = \frac{r_o}{\Delta} \frac{\sinh x_2 \sinh b(x_2-x_1) - b \cosh x_2 \cosh b(x_2-x_1)}{\cosh x_1} \tag{12}$$

$$z_{12} = z_{21} = -\frac{br_o}{\Delta} \tag{13}$$

$$z_{22} = -\frac{r_o}{\Delta} \frac{\sinh x_1 \sinh b(x_2-x_1) + b \cosh x_1 \cosh b(x_2-x_1)}{\cosh x_2} \tag{14}$$

where $b = \sqrt{1 + sr_oc_o}$ and

$$\Delta = b \sinh(x_2-x_1) \cosh b(x_2-x_1) - \cosh(x_2-x_1) \sinh b(x_2-x_1) - sr_oc_o \cosh x_1 \cosh x_2 \sinh b(x_2-x_1).$$

To simplify calculations, each of the four networks is depicted as a two-port "black box" characterized by these parameters. The actual values of the parameters for a given network are determined by its material composition, size, and shape. Since changes in material composition

and size produce proportional changes in all the open-circuit parameters, the characteristics of identically shaped networks of various sizes and compositions can be determined by studying one "normalized" network. However, the characteristics displayed by networks of different shapes are quite unique and have to be studied individually.

To overcome the obvious computational difficulties which arise from applying the relatively complex equation for the impedance parameters to the problem, a Burroughs B5500 digital computer will be utilized.

Figure 7 shows both the actual circuit subjected to this investigation and the "black box" representation used as a model for derivations.

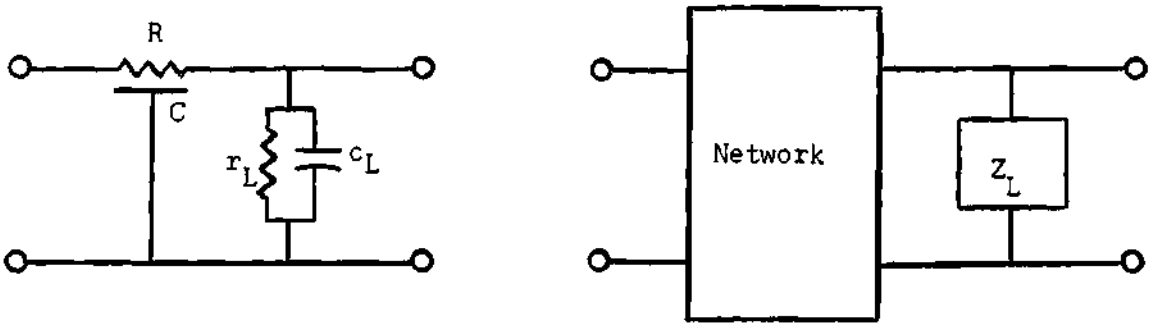

Figure 7. Schematic Diagram of Theoretical Circuits.

From this black-box representation, the following equation was derived which expresses the voltage-transfer characteristics of a network in terms of its open-circuit impedance parameters and the load impedance.

$$E_2/E_1 = \frac{z_{11}z_L}{z_{11}z_{22} + z_{11}z_L - z_{12}z_{21}} \qquad (15)$$

When each impedance parameter and the load impedance are represented by

the sum of their real and imaginary parts, ($Z_{ab} = R_{ab} + jX_{ab}$), the following equation is obtained.

$$\frac{E_2}{E_1} = \frac{[R_{12}R_L - X_{12}X_L] + j[R_{12}X_L + X_{12}R_L]}{[R_{11}(R_{22}+R_L)-X_{11}(X_{22}+X_L)-R_{12}^2+X_{12}^2]+j[R_{11}(X_{22}+X_L)+X_{11}(R_{22}+R_L)-2R_{12}X_{12}]} \tag{16}$$

For a parallel RC load R_L and X_L can be expressed in terms of the load resistance r_L, the load capacitance c_L, and the frequency variable ω.

$$R_L = \frac{r_L}{1 + \omega^2 r_L^2 c_L^2} \tag{17}$$

$$X_L = \frac{-\omega r_L^2 c_L}{1 + \omega^2 r_L^2 c_L^2} \tag{18}$$

An examination of the equations for the open-circuit impedance parameters on pages 10 and 11 reveals that it would be difficult to resolve them into their real and imaginary parts. The following listing outlines the general method which proved to be the most effective approach to this problem:

(1) Begin by assigning dummy variables to the real and imaginary parts of the most elementary variables of the equation.

(2) Express the next most elementary variables of the equation in terms of these dummy variables.

(3) Separate these expressions into real and imaginary parts

and assign new dummy variables to each of these parts.

(4) Continue this process sequentially until the final expressions are obtained.

The above method proves to be very adaptive to computer programming techniques and is used through the problem.

An examination of the equation for the voltage-transfer functions reveals that they are expressed in terms of the following variables:

(1) the load resistance,

(2) the load capacitance,

(3) the individual network parameters (α, λ, x_1, x_2, r_o, c_o), and

(4) the frequency variable ω.

The major part of this research involves the study of the effects of changes in some of these variables on the terminated voltage-transfer characteristics of various networks.

CHAPTER II

METHODS OF ANALYSIS AND COMPARISON

Before a quantitative study of tapered RC thin-film networks can be attempted, some standard for comparison must be established. The necessity of such a standard becomes apparent when the open-circuit characteristics of a large number of dissimilar lines are compared and found to differ quite noticeably. These characteristics are functions of the individual physical parameters of the networks, and within certain limitations, an infinite number of combinations of these parameters exist for each type of network. It is obvious that the comparison of an infinite number of RC lines in any respect would have been virtually impossible. A comparison of the effects of load on the terminated voltage-transfer characteristics of different networks would have been both impracticable and meaningless if their open-circuit characteristics are quite different. Therefore, a criterion has to be established for selecting specific physical parameters to describe individual networks from the four general classes.

Preliminary studies of various RC lines revealed that many lines display very similar open-circuit-voltage-transfer characteristics. Although for all practical purposes, the differences among these characteristics are not discernible, the networks themselves can not be considered identical. In fact, these similar lines can possibly differ quite noticeably in other respects such as their asymptotic performance at high frequencies, their behavior with load, etc. However, this marked similarity

of open-circuit characteristics provides the groundwork on which the selection of specific networks for this investigation is based. By selecting for comparison only networks with essentially identical low-frequency open-circuit-voltage-transfer characteristics, a quantitative investigation of the effects of load is made possible.

Therefore, a necessary precedence to the primary investigation is a critical examination of the open-circuit characteristics of the four types of networks. From this investigation, a precise criterion for judging two or more networks similar can be established. This criterion is put in the form of the following definition.

> All open-circuit-voltage-transfer characteristics are normalized such that their 3-db-loss points (ω_1) coincide. After this normalization, all lines that have identical 30-db-loss points are said to <u>resemble</u> each other.

Figures 8a and 8b illustrate the similarity of the normalized open-circuit-magnitude and phase characteristics of three resembling lines.

If the <u>low-frequency-cut-off ratio</u> (L.F.C.R.) for a network is defined from its open-circuit-voltage-transfer characteristics to be the ratio of the 30-db-loss frequency (f_2) to the 3-db-loss frequency (f_1), it becomes obvious that <u>resembling lines</u> are those that have the same <u>low-frequency-cut-off ratio</u>. This definition of resembling lines will be used as a determinant in the selection of physical parameters for the lines that are studied. The general method used in applying this determinant quantitatively is described below.

The open-circuit-voltage-transfer function of any linear bilateral

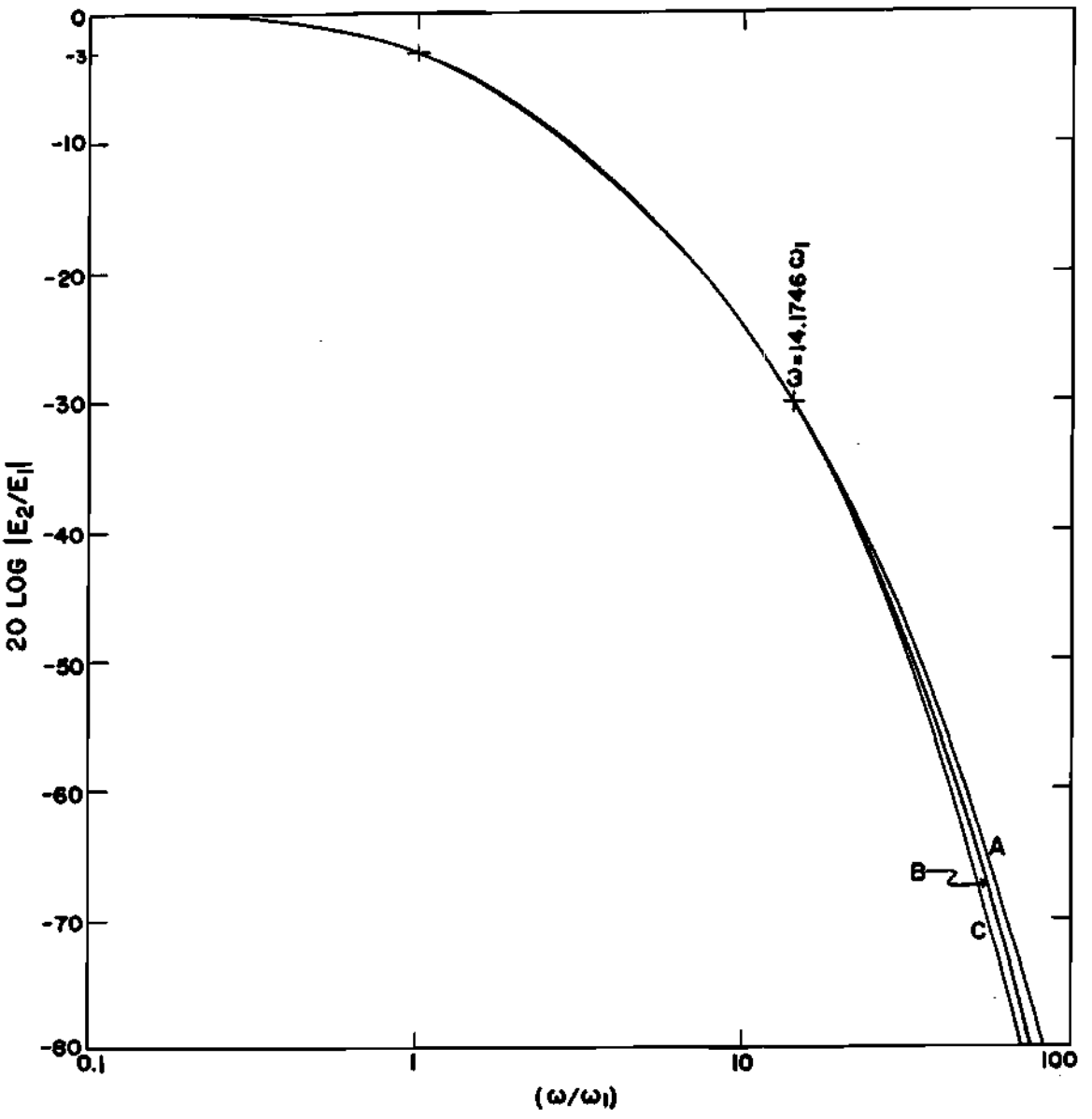

Figure 8a. Normalized Magnitude Characteristics of Three Resembling Lines

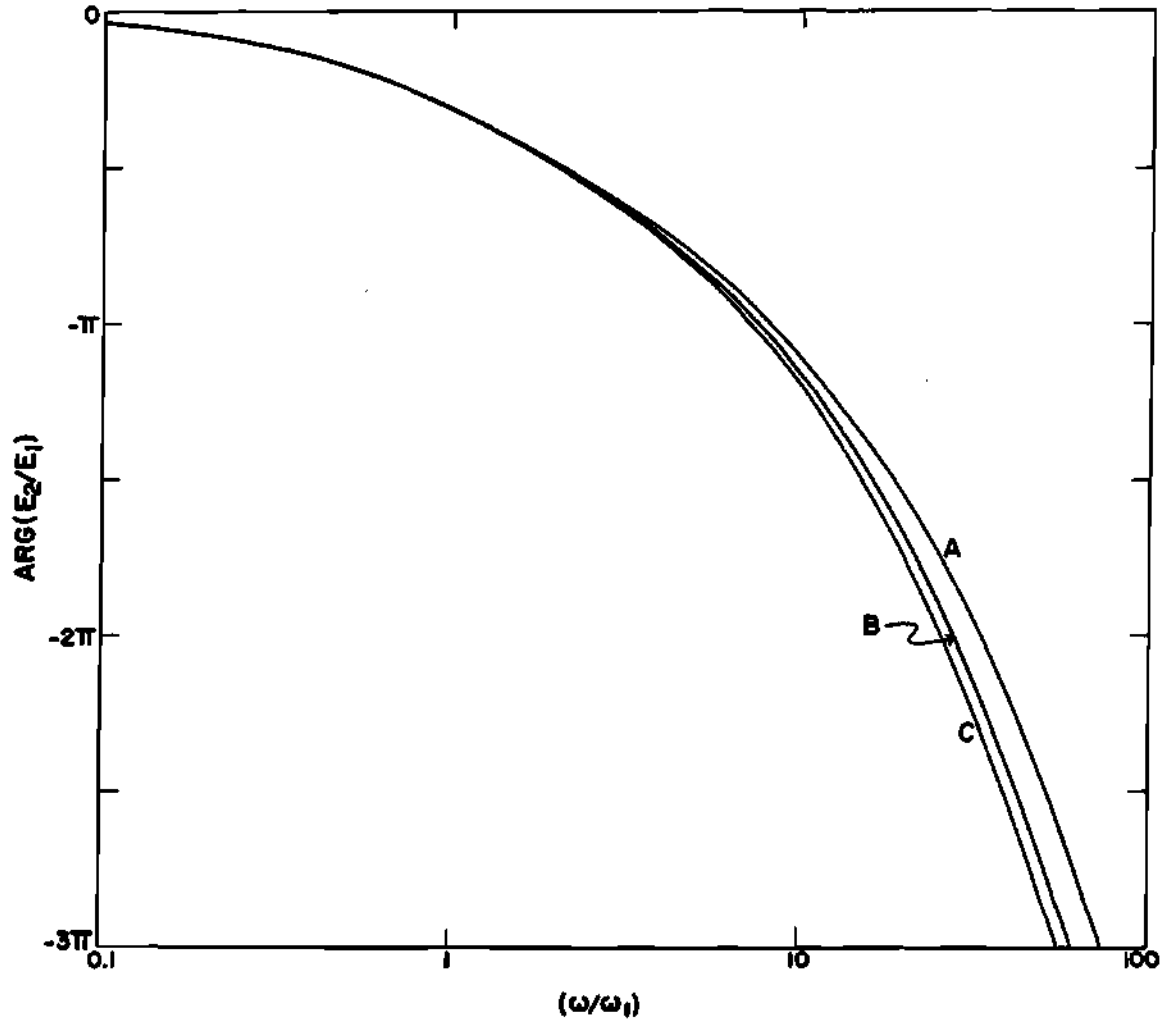

Figure 8b. Normalized Phase Characteristics
of Three Resembling Lines

two port network can be expressed in terms of its open-circuit impedance parameters by the following equation from classical circuit theory:

$$E_2/E_1 = z_{21}/z_{11} \tag{19}$$

The above expression, the equations for z_{11} and z_{21} on pages 10 and 11, and the method of substitution outlined in Chapter 1 are utilized in devising computer programs that express the open-circuit-voltage-transfer characteristics of each of the four types of networks in terms of their individual physical parameters and the frequency variable ω. By using these programs to generate data for vast combinations of physical parameters, and plotting curves from this data, it would conceivably have been possible to determine the values of the physical parameters for each type of network that produced resembling lines. Obviously this method would have been both inefficient and inaccurate. Because of the complexity of the expressions for the voltage-transfer characteristics, an implicit solution for the physical parameters of a network in terms of its low-frequency-cut-off ratio would also prove to be highly impractical.

However, through an application of Newton's Method of approximation (4) and an interpolation procedure, a general solution to this problem has been devised. This general solution, which is outlined below, is then put in the form of a computer program and used in conjunction with the programs discussed earlier to determine the physical parameters of networks with specific low-frequency-cut-off ratios.

1. Select the desired low-frequency-cut-off ratio.
2. Assume trial values for the following
   (a) 3-db-loss point (ω_1)

(b) 30-db-loss point (ω_2)

(c) physical parameters (a, λ, x_1, x_2, etc.).

3. Determine the 3-db-loss point (ω_1) by utilizing Newton's Method of Approximation to find the root of the following equation.

$$\left|\frac{E_2(\omega)}{E_1(\omega)}\right|_{db} = -\ 3db \qquad (20)$$

where (a) $|E_2/E_1|$ is calculated using previously derived computer programs.

(b) The approximation method begins with the assumed value of ω_1 and improves on its accuracy until adequate precision is obtained.

4. Similarly determine the 30-db-loss point (ω_2).

5. Calculate the low-frequency-cut-off ratio ω_2/ω_1 and record it along with the corresponding physical parameters which were assumed.

6. Assuming new trial values of physical parameters, repeat steps 3, 4, and 5 until a general trend has been established and recorded.

7. From this recorded data, use interpolation to choose new trial physical parameters and then calculate the low-frequency-cut-off ratio using these parameters.

8. Repeat interpolation of the values for the physical parameters and calculation of corresponding low-frequency-cut-off ratios until desired accuracy is obtained.

A preliminary study of the relationship of the physical parameters of a network to its open-circuit performance has revealed that the low-frequency-cut-off ratio is invariant with respect to several parameters. As stated in Chapter 1, the incremental values of resistance and capacitance along the length of the four types of lines chosen for this study are expressed in terms of the constants r_o and c_o and specific functions of the displacement from the origin of the coordinate systems in which the lines are described. For a specific type of network, the values of r_o and c_o determine its material composition, thickness, and width. The shape of the network is determined by its descriptive equations, the location of its input and output ports, and the choice of scale used for measurement. Once the shape of a network has been fixed, changes in either its material composition, width, or thickness produce only variations in r_o and c_o and thus result in proportional changes in all of the incremental values of resistance and capacitance. Variations in the overall length of the line serve only to change the scale used for measurement and also result in proportional changes in these incremental values.

As in a lumped RC network, proportional changes in all the capacitive and/or resistive elements result in a frequency scaling of its open-circuit-voltage-transfer characteristics. Since the actual shape of these characteristics is not altered, the low-frequency-cut-off ratio is unaffected. That is, for an RC transmission line the low-frequency-cut-off ratio is dependent only on the ratio of the incremental values resistance and capacitance and not on their absolute magnitudes. Therefore, in determining the physical parameters of a network with a specific low-frequency-cut-off ratio, only parameters which affect its

actual shape are considered. Also, the characteristics of identically shaped networks of various sizes and compositions can be determined by studying one normalized network. Mathematical verification of these conclusions can be obtained through a manipulation of the equations for the open-circuit impedance parameters of the four networks on pages 10 and 11. When it can be shown that each of the four parameters is a linear function of a specific variable, then that variable is not a determining factor of the low-frequency-cut-off ratio.

Since the incremental resistance and capacitance along the length of the uniform line are constant by definition, the shape of this line is always rectangular. Therefore, the low-frequency-cut-off ratio for the uniform line is invariant with respect to all of its physical parameters. This ratio was calculated from normalized open-circuit-voltage-transfer characteristics and found to be equal to 14.174593.

If the substitutions $s' = sr_o c_o \lambda^2$ and $N = \alpha\lambda$ are made in the equations for the open-circuit impedance parameters of the exponential line, each parameter becomes a linear function of r_o and λ and a non-linear function of only N and s. Therefore, if the quantity $\alpha\lambda$, which represents the degree of taper, is considered as one variable physical parameter, it becomes the only determining factor of the low-frequency-cut-off ratio for the exponential line. Figure 9 shows the relationship between this ratio and $\alpha\lambda$, and Table 1 gives the values of $\alpha\lambda$ for exponential lines with integer cut-off ratios. This data has been calculated using the outlined method discussed on pages 19 and 20. It should be noted that for $\alpha = 0 (\alpha\lambda = 0)$ the exponential line becomes a uniform line with the corresponding cut-off ratio of 14.1746.

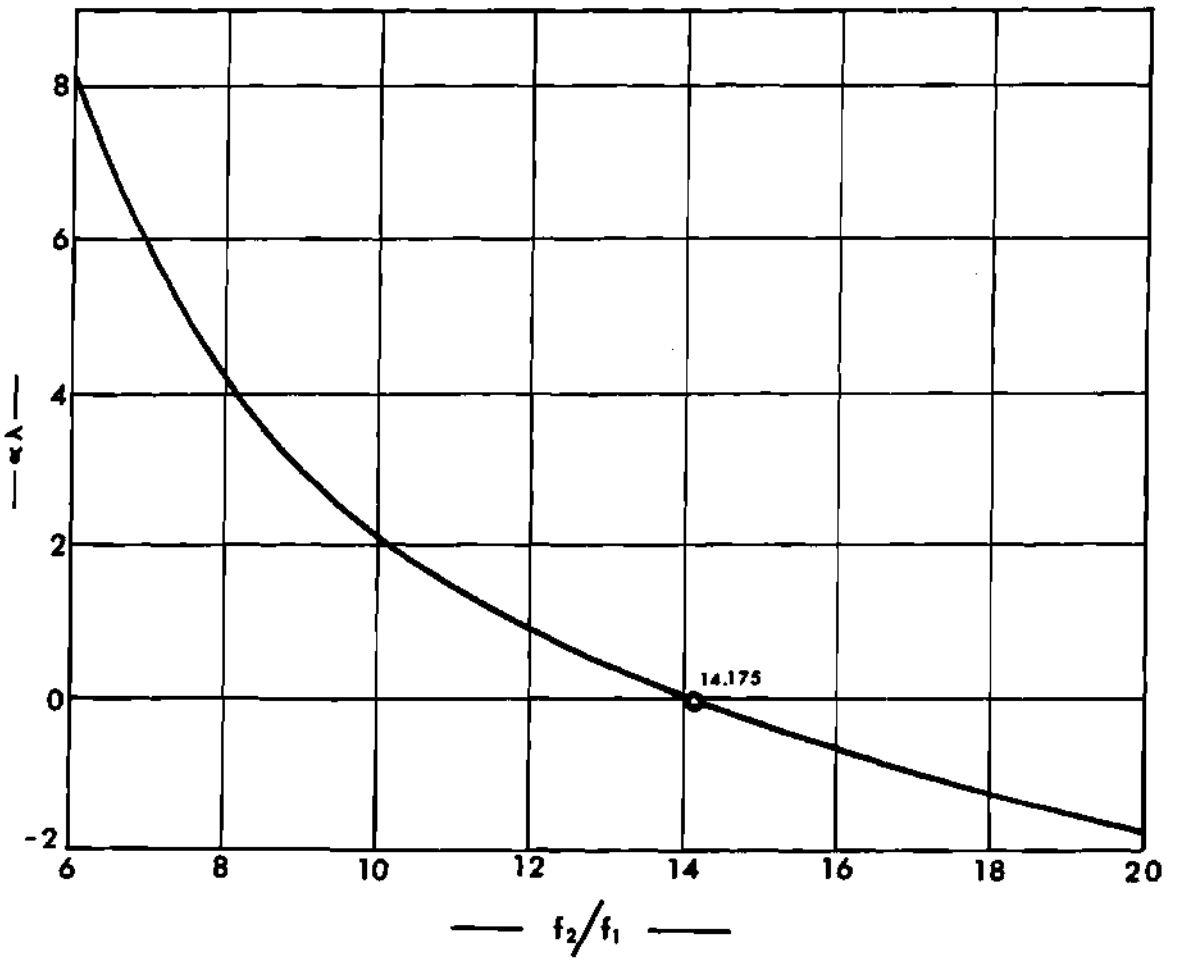

Figure 9. Variation in The Low-Frequency-Cut-Off Ratio for Exponential RC Lines

Table 1. Values of $\alpha\lambda$ Which Produce Exponential Lines With Integer Cut-Off Rates

Low-Frequency Cut-Off-Ratio ω_2/ω_1	Degree of Taper $\alpha\lambda$	ω_1 (Multiply by $1/r_0 c_0 \lambda^2$)
6	8.17756	18.10890
7	5.66067	11.84338
8	4.10056	8.52120
9	3.00722	6.49321
10	2.17777	5.13989
11	1.51332	4.17996
12	0.95975	3.46820
13	0.48483	2.92236
14	0.06795	2.49244
14.1746	0	2.42669
15	-0.30481	2.14641
16	-0.64328	1.86277
17	-0.95474	1.62664
18	-1.24478	1.42734
19	-1.51786	1.25707
20	-1.77769	1.10995

The substitution $s' = sr_o c_o$ in the equations for the open-circuit impedance parameters of both the trigonometric and the hyperbolic lines reveals that the location of the input and output ports determine the low-frequency-cut-off ratio for these lines. Therefore, the outlined procedure is applied to the problem of determining the values of x_1 and x_2 for lines with specific cut-off ratios. Since there are multitudes of such combinations, these parameters are best presented in the form of contour maps as shown in Figure 10 for the trigonometric line and Figure 11 for the hyperbolic line. In these graphs, values of x_1 and x_2 that lie on contours of the same low-frequency-cut-off ratio produce networks that all have resembling open-circuit-voltage-transfer characteristics.

Unlike the exponential line, there are virtually an infinite number of different trigonometric and hyperbolic lines with each cut-off ratio. When the range of values of x_1 and x_2 for any specific group of resembling lines is considered, the wide variation in the shape of these lines is evident. Note that proper choices of these parameters produce networks which resemble the uniform line with low-frequency-cut-off ratios of 14.1746.

A re-examination of Figures 8a and 8b reveals how similarly resembling lines behave at open circuit. These curves correspond to three RC lines of vastly different shapes. Characteristics A are for a uniform line; characteristics B are for a trigonometric line with $x_1 = 0.6142$ and $x_2 = 3.1400$; characteristics C are for a hyperbolic line with $x_1 = -5.00$ and $x_2 = 1.78403$. Lines B and C correspond to two extreme points on the dotted contours of Figures 10 and 11. All characteristics which correspond to other points on these contours are expected to lie between the curves C and A of Figure 7. It is seen that even if the variations of r

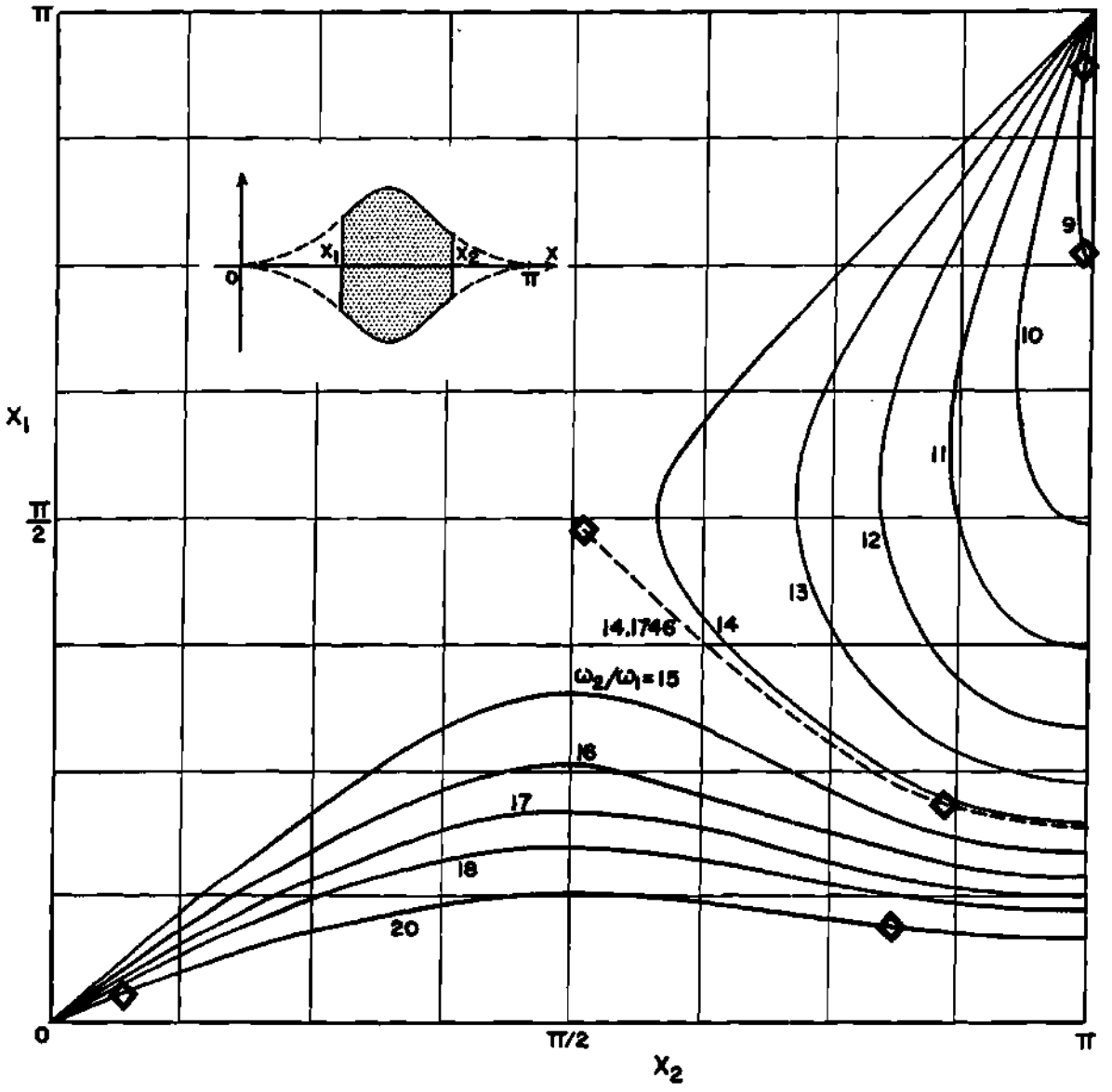

Figure 10. Contours of Resembling Trigonometric RC Lines

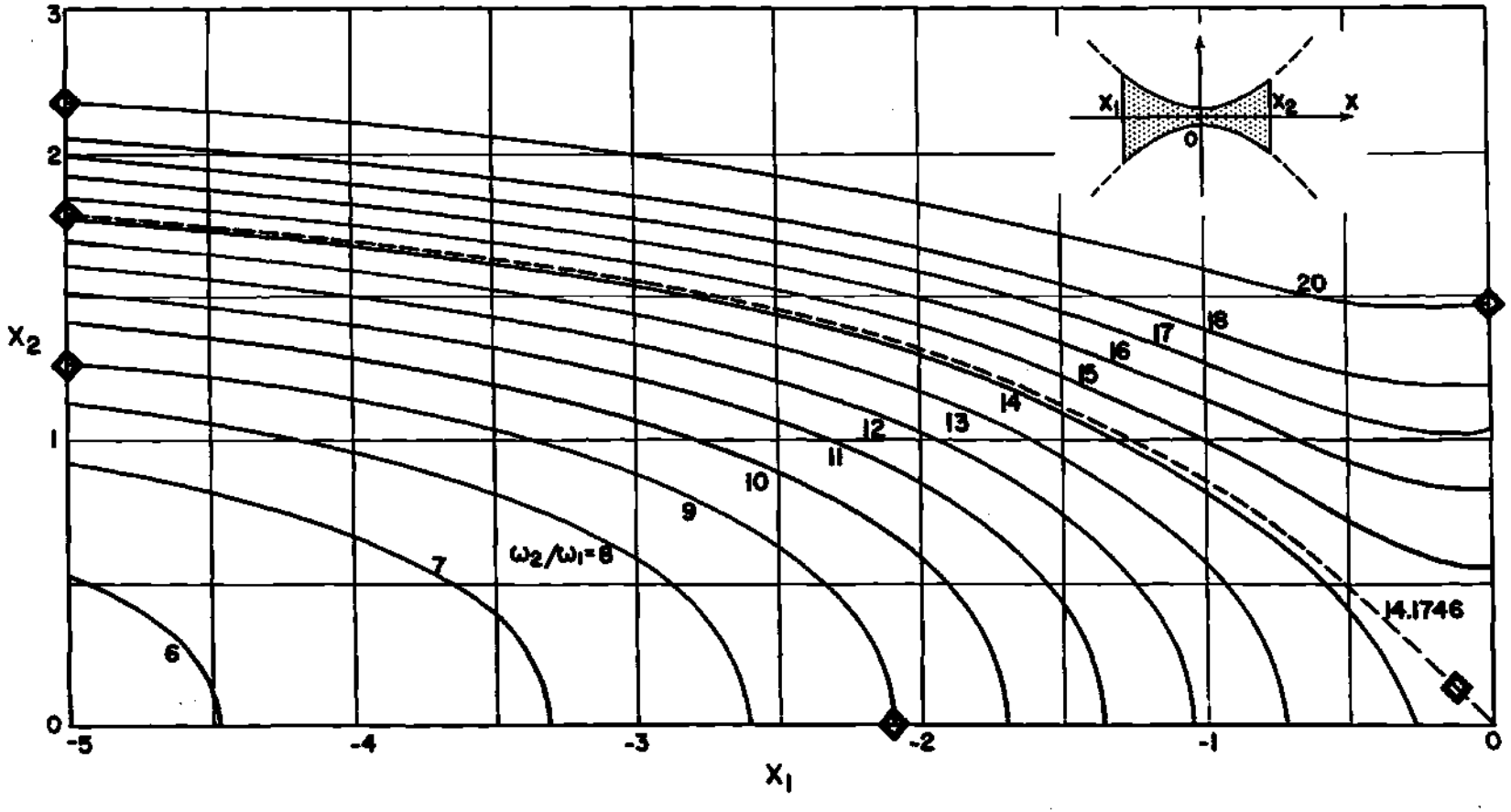

Figure 11. Contours of Resembling Hyperbolic RC Lines

and c are very different, RC lines can be constructed which perform comparably under open-circuit conditions.

Before the quantitative methods discussed in Chapter 1 can be applied to the problem of studying the effects of load on these resembling lines, one minor difficulty has to be overcome. Even though the lines used for comparison have almost identical normalized low frequency performance, their total values of resistance and capacitance differ significantly. When one realizes that each normalized network represents an infinite number of networks of various sizes and material compositions, this difficulty is even more apparent.

If a specific load with discrete component values is connected to a number of resembling lines, a comparison of their performance would be meaningless since the magnitude of such a load with respect to the total values of resistance and capacitance of each line would be quite varied. Therefore, some method of load normalization has to be devised.

The normalized load conductance G_N is defined as the ratio of the actual load conductance to the total value of conductance of the network being studied. That is:

$$G_N \triangleq \frac{g_L}{G_T} \tag{21}$$

The total value of conductance for a specific line can be calculated by integration from the equations of the resistance variation along the line, using the location of the input and output ports as limits of integration.

Also, the normalized load capacitance P is defined as the ratio of the susceptance of the load capacitance at the frequency where the open circuit attenuation of the network being studied is 30 db to the actual load conductance. That is:

$$P \triangleq \frac{C_L \times \omega_{2oc}}{g_L} \tag{22}$$

Using the above load normalization and the definition of resembling lines as a criterion for the selection of lines to be studied, a quantitative comparison of the effect of load is possible. The results of this comparison are presented in the following chapter.

CHAPTER III

THEORETICAL RESULTS AND CONCLUSIONS

As stated in Chapter 1, the objective of this research is to determine the proper shaping of RC thin-film networks that are terminated in parallel resistance-capacitance loads. The definition of resembling lines provides a criterion for selection of the specific networks to be studied. It has been decided to limit the investigation to three groups of resembling lines, those with low-frequency-cut-off ratios of 9, 14.175, and 20. This limitation makes possible a representative study of variously shaped thin-film networks without unnecessary repetition. The cut-off ratio of 14.175 is chosen so that the uniform line will be included in the investigation. Choice of the ratios 9 and 20 provides for comparison exponential, trigonometric and hyperbolic lines with cut-off ratios approaching practical limits.

It is the primary aim of this research to determine, through a comparison of the performance of the four types of lines chosen, the general shape that a RC thin-film network should have for optimum performance under terminated conditions. The uniform lines, the two exponential lines with cut-off ratios of 9 and 20, and the multitude of trigonometric and hyperbolic lines with the three chosen cut-off ratios provide an unlimited supply of variously shaped networks for this comparison.

Using the outlined procedures discussed in Chapter 1, equations (16), (17), (18), (21), and (22) along with the equations for the open

circuit impedance parameters on pages 10 and 11, have been utilized to devise four computer programs that express the terminated voltage-transfer characteristics of each general type of network in terms of its physical parameters and the normalized load parameters.

The actual values of the physical parameters for each network are explicitly determined from the low-frequency cut-off ratio specifications and the curves and contours of Chapter 2 (Figures 9, 10, and 11). Once the networks have been specified by these parameters, their voltage-transfer characteristics for different terminations are determined by varying the values of the normalized load parameters in the computer programs.

The effects of these terminations on the performance of a particular network are first studied by investigating the changes that take place in the shape of its normalized voltage-transfer characteristics when these load parameters are increased in discrete steps. Obviously, one initial effect on these characteristics resulting from the addition of a resistance load is the introduction of a dc attenuation. The value of this attenuation depends on the relative size of the load with respect to the total conductance of the network. For instance, a load conductance equal to the total conductance results in an attenuation of 6 db. Of course, there is a specific value of load conductance for each network that gives a dc attenuation of 30 db. This value is designated as G_{L30db} and it is easily determined as:

$$G_{L30db} = (1 + 10^{1.5})G_T \qquad (23)$$

or

$$G_{L30db} = 32.6G_T \tag{24}$$

The above observations make possible a more convenient and meaningful method of normalizing the load conductance with respect to the total conductance of the network. The normalized load conductance G_N defined in equation 21 is not meaningful since it is defined in terms of the unfamiliar total conductance G_T. However, a new normalized conductance G defined as the ratio of the actual load conductance g_L to the load conductance that produces a 30-db-dc attenuation, G_{L30db}, that is

$$G = \frac{g_L}{G_{L30db}} \tag{25}$$

is more realistic than G_N. And since G_{L30db} differs from G_T by only a constant multiplier, the above equation provides for the required load normalization. This equation is solved for the actual load conductance g_L in terms of G and G_{L30db} and incorporated in previously derived computer programs. Obviously, G_{L30db} has to be calculated for each network. The computer programs are essentially numerical solutions of the normalized circuit shown below for the magnitude of E_2/E_1 in db versus a normalized frequency variable. They have been used to compute the voltage transfer characteristics of resembling lines terminated in various loads.

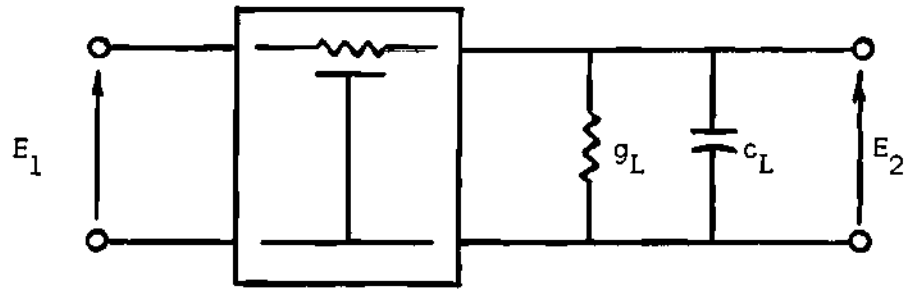

Where: $g_L = g \times G_{L30db}$

$$c_L = \frac{P \times g_L}{\omega_{2oc}}$$

Figure 12. Normalized Theoretical Circuit.

For example, the uniform line, a resembling trigonometric line ($x_1 = 0.700$, $x_2 = 2.684$), and a resembling hyperbolic line ($x_1 = -5.000$, $x_2 = 1.784$) have been first selected for study. The particular combinations of x_1 and x_2 for the trigonometric and hyperbolic lines are specifically chosen to provide for comparison three networks with vastly different shapes. A scale model drawing of each of these lines is depicted in Figure 13. The extreme difference in the general variation of the incremental values of resistance and capacitance for the three networks should be noted. The resistance of the trigonometric line is high at the input and output ports and low in the area between them; the resistance of the uniform line is constant; and the resistance of the hyperbolic line is low at both the input and output ports and high in the area between them. The corresponding capacitance variations for the three networks are required by definition to be opposite to their resistance variations.

To observe the similarity of the open-circuit performance of these

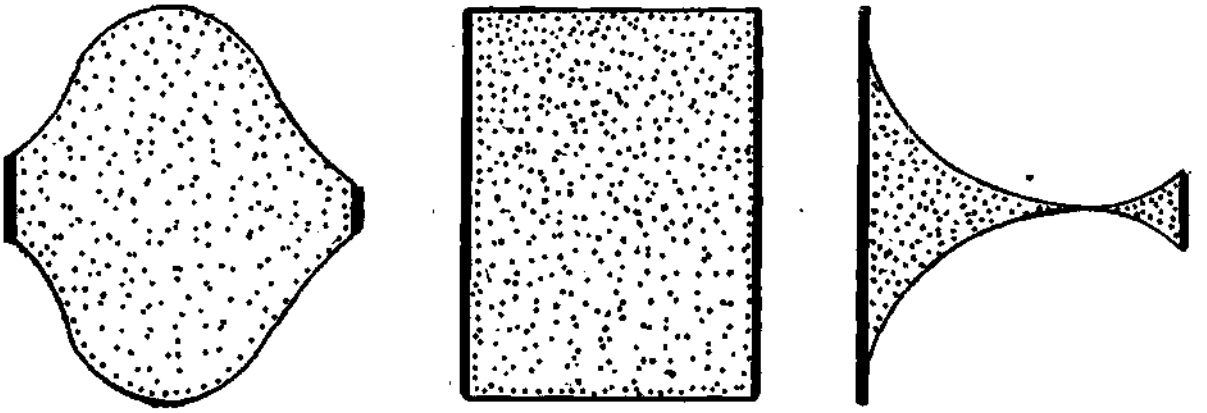

Trigonometric Uniform Hyperbolic

Figure 13. Scale Model Drawing of Three Networks.

three lines, their normalized voltage-transfer characteristics are determined after equating both of the normalized load parameters to zero. Figure 14 depicts these characteristics in graphical form. The frequency variable has been normalized with respect to the open-circuit-30-db attenuation frequency f_{2oc} and plotted on a logarithmic scale. The reason for the choice of f_{2oc} rather than f_{1oc} as the reference frequency for normalization will become apparent later. It should be noted that as required by the definition of resembling lines, the three curves all pass through identical 3 db and 30 db points, and that for levels of attentuation less than 60 db, they are almost identical.

The effect of a simple resistance termination on the open circuit characteristics of these three networks is first studied by investigating the changes in the shape of these curves resulting from several discrete values of normalized load conductance. For simplicity, only changes in the

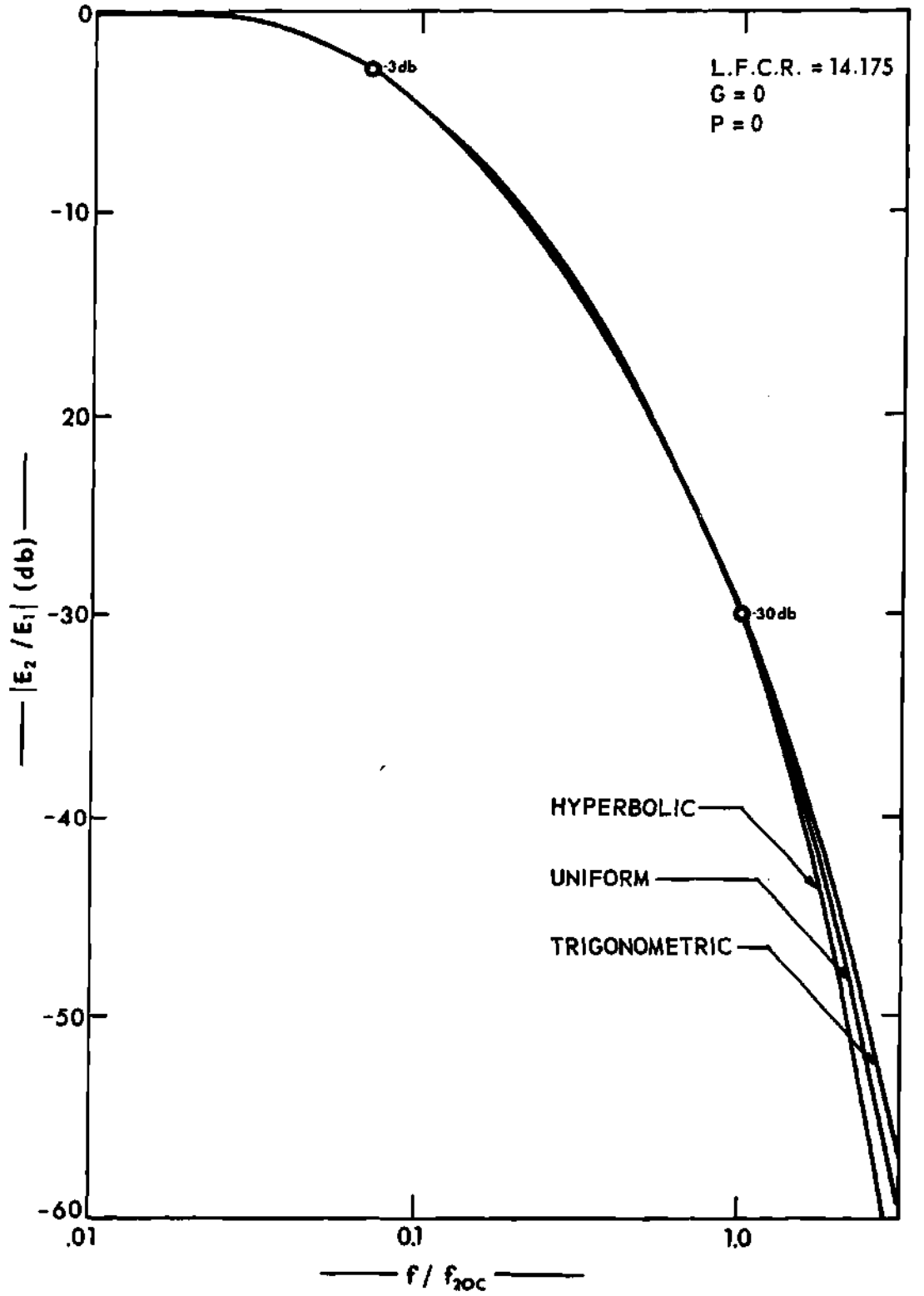

Figure 14. Normalized-Open-Circuit-Voltage-Transfer Characteristics of Three Resembling Lines, L.F.C.R. = 14.175

curve for the trigonometric line are first considered. Figure 15 depicts the original open-circuit-voltage-transfer characteristics for this trigonometric line along with its terminated characteristics resulting from the terminations: G = 0.2, G = 0.5, and G = 1.0. The increased dc attenuation which resulted from loading is quite evident in this figure. It should also be noted that for G = 1, this attenuation is 30 db as defined. More important, Figure 15 illustrates that as the load resistance is increased, the resulting voltage-transfer characteristics move further and further away from the open circuit chatacteristics.

The effects of the introduction of a parallel capacitance in the load circuit of this same trigonometric line are studied next by increasing the normalized load capacitance in discrete steps while holding the load conductance constant. The results of such an investigation for G = 0.2 and P = 0, 5, and 10 are displayed in graphical form in Figure 16. It can be seen that the addition of parallel capacitance in the load circuit results in additional shift in the voltage-transfer characteristics away from the open-circuit curve.

Figures 15 and 16 illustrate the general effect that a parallel resistance-capacitance termination has on the voltage-transfer characteristics of each of the thin-film networks studied throughout this investigation. However, the amount by which these characteristics are shifted for a specific load varies considerably for different networks. By superimposing the terminated voltage-transfer characteristics of several lines on the same graph, the shift in these characteristics can be compared. The results of such comparisons provides the foundation on which the conclusions of this research will be based.

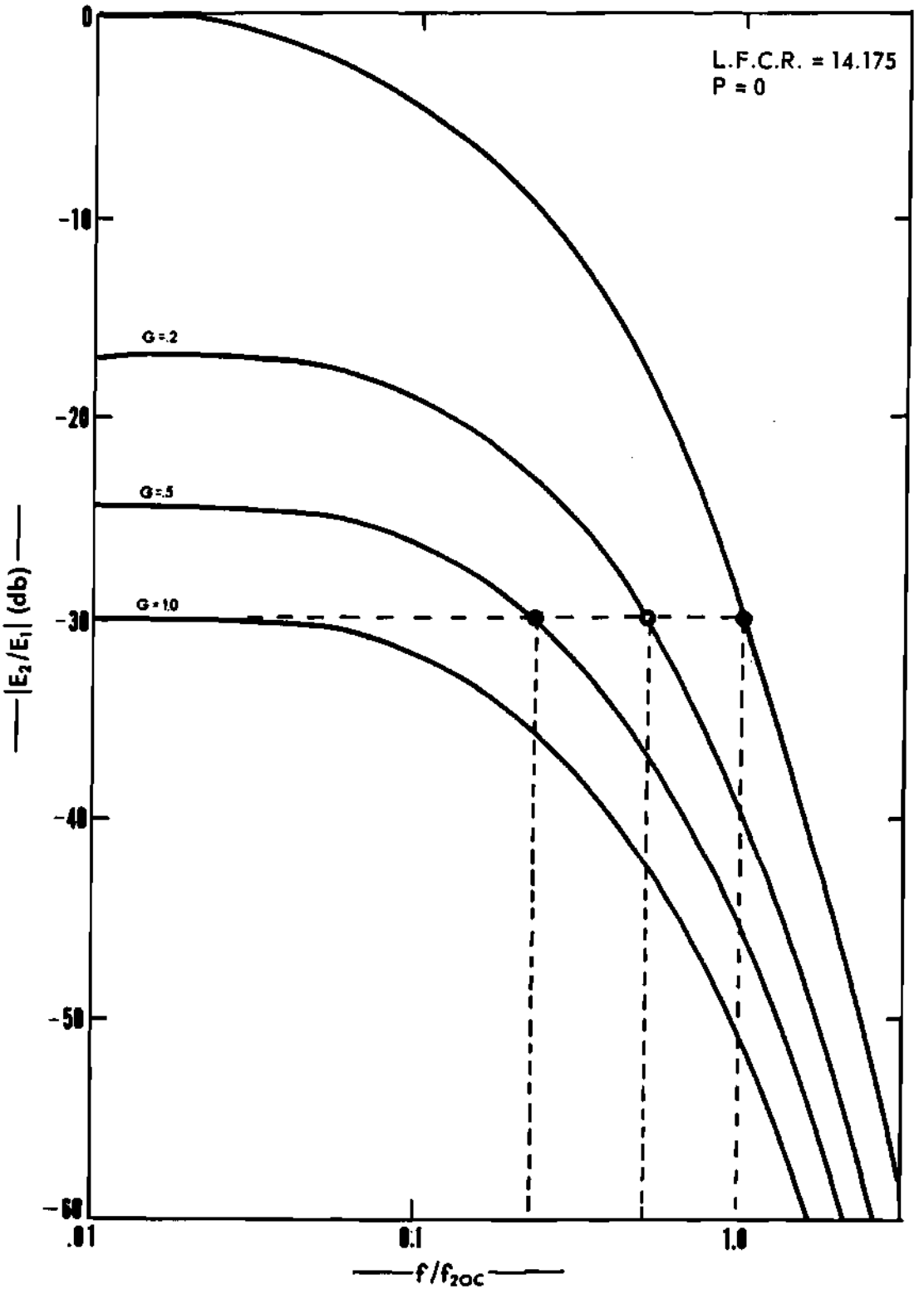

Figure 15. Normalized-Terminated-Voltage-Transfer Characteristics of a Trigonometric RC Line, L.F.C.R. = 14.175

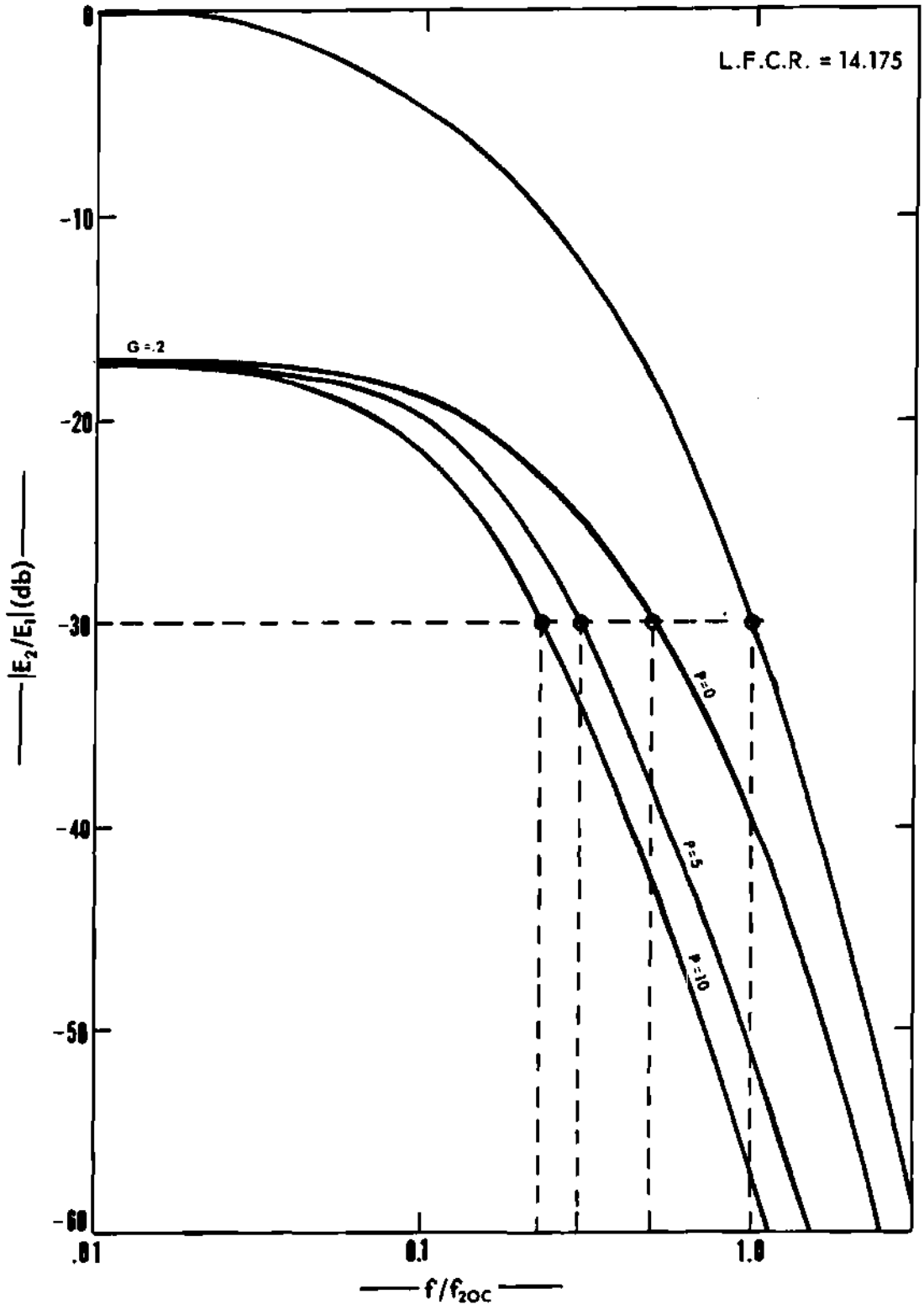

Figure 16. Normalized-Terminated-Voltage-Transfer Characteristics of a Trigonometric RC Line, L.F.C.R. = 14.175

For example, the curves of Figures 16 and 17 for the trigonometric line are examined along with similar curves for the uniform and hyperbolic lines. A combination of two sets of these transfer characteristics is depicted in Figure 17 along with one curve representing the open-circuit characteristics of all three lines.

The solid curves represent the voltage-transfer characteristics of the three networks terminated in purely resistive loads (G = 0.5), and the broken curves depict the changes which result when large load capacitances, (P = 10), are introduced. In both cases the curves for the hyperbolic line remain much closer to the original open-circuit curve. Therefore, the theoretical performance of these specific networks and terminations agrees with the expectations. That is, since the hyperbolic line has a considerably lower relative impedance at the output port than either the uniform or trigonometric lines, it had been predicted that its voltage-transfer characteristics would not be as susceptible to load changes.

However, before any general conclusions can be made, this prediction need be verified for numerous combinations of networks and terminations. Conceivably, the above process of comparing the shape of voltage-transfer characteristics could have been continued until a definite trend had been established. Even though this method could have produced adequate results, it would have been limited to specific networks and certain discrete terminations. It also would have required an impractical amount of time and work. Therefore, a search was made for a more efficient method of investigation that would make possible the comparison of an unlimited number of different networks terminated in all practical values of parallel resistance and capacitance.

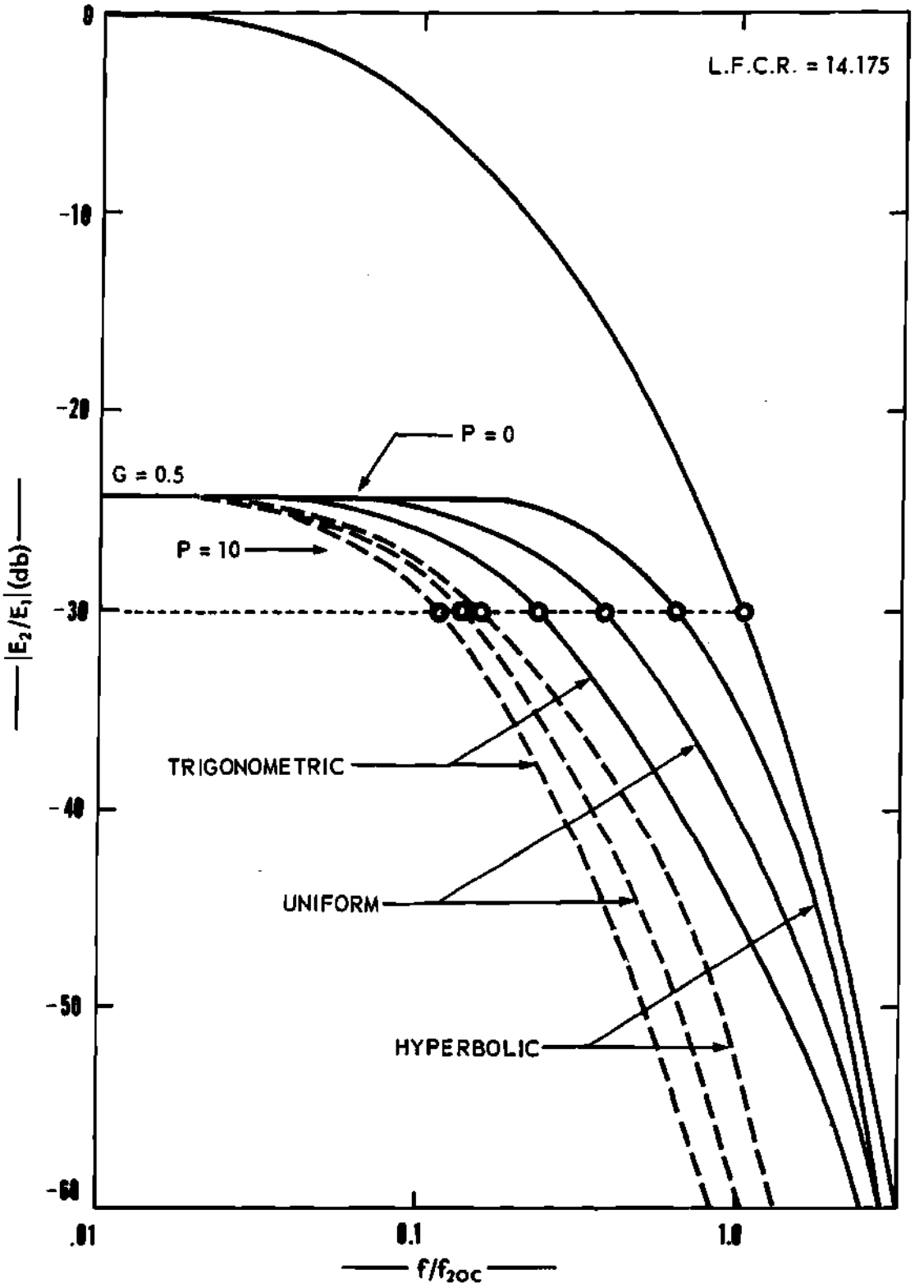

Figure 17. Normalized Terminated-Voltage-Transfer Characteristics of Three Resembling RC Lines, L.F.C.R. = 14.175

An examination of the curves of Figures 15, 16, and 17 reveals that the 30-db-attenuation frequency for each curve is a good indicator of its relative position with respect to other curves. The shift in the normalized 30-db frequency from its open-circuit value of 1 is commensurate with the effect of increased loading on the shape of a particular curve. Therefore, for a specific load, the relative performance of resembling networks can be compared by simply examining their normalized 30-db-attenuation frequencies. Obviously, this method is not applicable for loads which produce a dc attenuation greater than 30 db. However, it does provide a means of continuously comparing the effects of all practical loads.

For example, a re-examination of the curves of Figure 15 for a trigonometric line terminated in a simple conductance reveals that as the normalized conductance G is increased from zero to one, the corresponding normalized 30 db attenuation frequency f/f_{2oc} decreases from one to zero. Continuous plots of this frequency shift versus load graphically display the effects of simple resistance loading on this specific line. When similar curves for the uniform and hyperbolic lines are superimposed on the same graph (Figure 18), a very effective comparison of their terminated performance is possible. Several key points on Figure 18 are marked for identification with specific voltage-transfer characteristics from Figures 15 and 17. For instance, the characteristic curve for the trigonometric line terminated in a normalized load conductance of 0.5 (Figure 15) passes through the 30 db attenuation line for a normalized frequency of 0.234. This particular voltage-transfer characteristic curve is represented in Figure 18 as the point G = 0.5, $f_2/f_{2oc} = 0.234$.

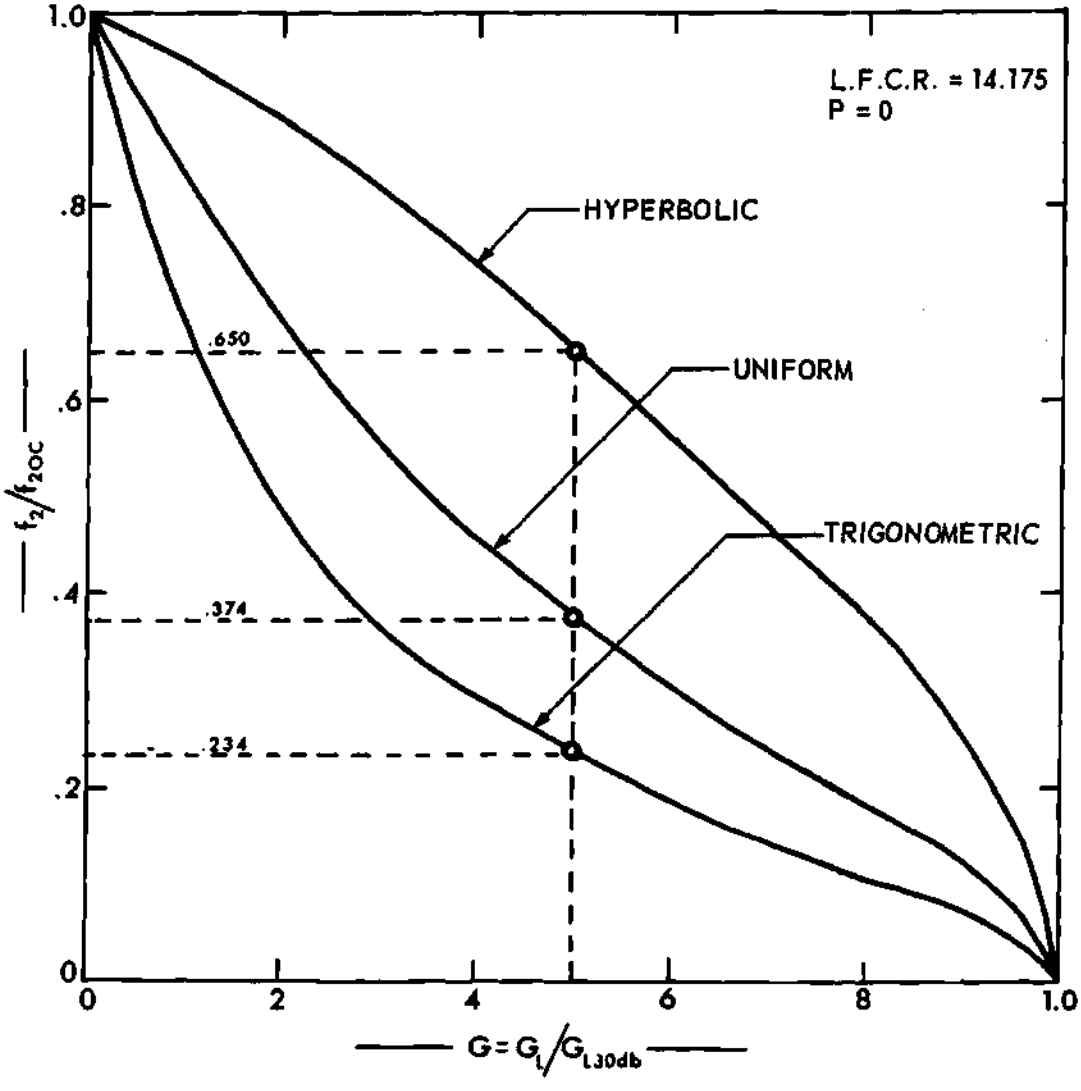

Figure 18. Shift in f_2/f_{2oc} Resulting From Loads With Constant P(P=0) and Variable G for 3 Resembling Lines, L.F.C.R. = 14.175

It should be obvious that each point on the curves of Figure 18 represents the voltage-transfer characteristics of a specific network with a specific termination. And since each curve of Figure 18 is a collection of such points for different resistance terminations, it represents the transfer characteristics of one network for all practical resistive loads. In each case the normalized frequency variable representing these characteristics decreases from one to zero as the normalized load conductance is increased from zero to one.

A comparative examination of the curves of Figure 18 reveals that for each value of the normalized load conductance, the corresponding normalized 30-db-attenuation frequency for the hyperbolic line is greater than that for either the uniform or trigonometric lines. Therefore, the conclusions for one specific resistive load based on a study of Figure 17 can be extended to include all practical resistive loads.

The shift in the voltage-transfer characteristics of these three networks resulting from the addition of parallel capacitances in their load circuits is also studied by comparing their normalized 30-db-attenuation frequencies. Curves of f_2/f_{2oc} versus G_L/G_{L30db} as in Figure 18 are first plotted for certain discrete values of normalized capacitance P. The changes in the curves of Figure 18 resulting from the addition of normalized load capacitances P = 1 and P = 10 are illustrated in Figures 19 and 20. It is obvious that for each value of load conductance, the corresponding 30-db-attenuation frequency is reduced when each of these two capacitances is included in the load circuit. More important, however, is the fact that the relative position of the three curves remains the same for every load combination. Again as in Figure 18, each point

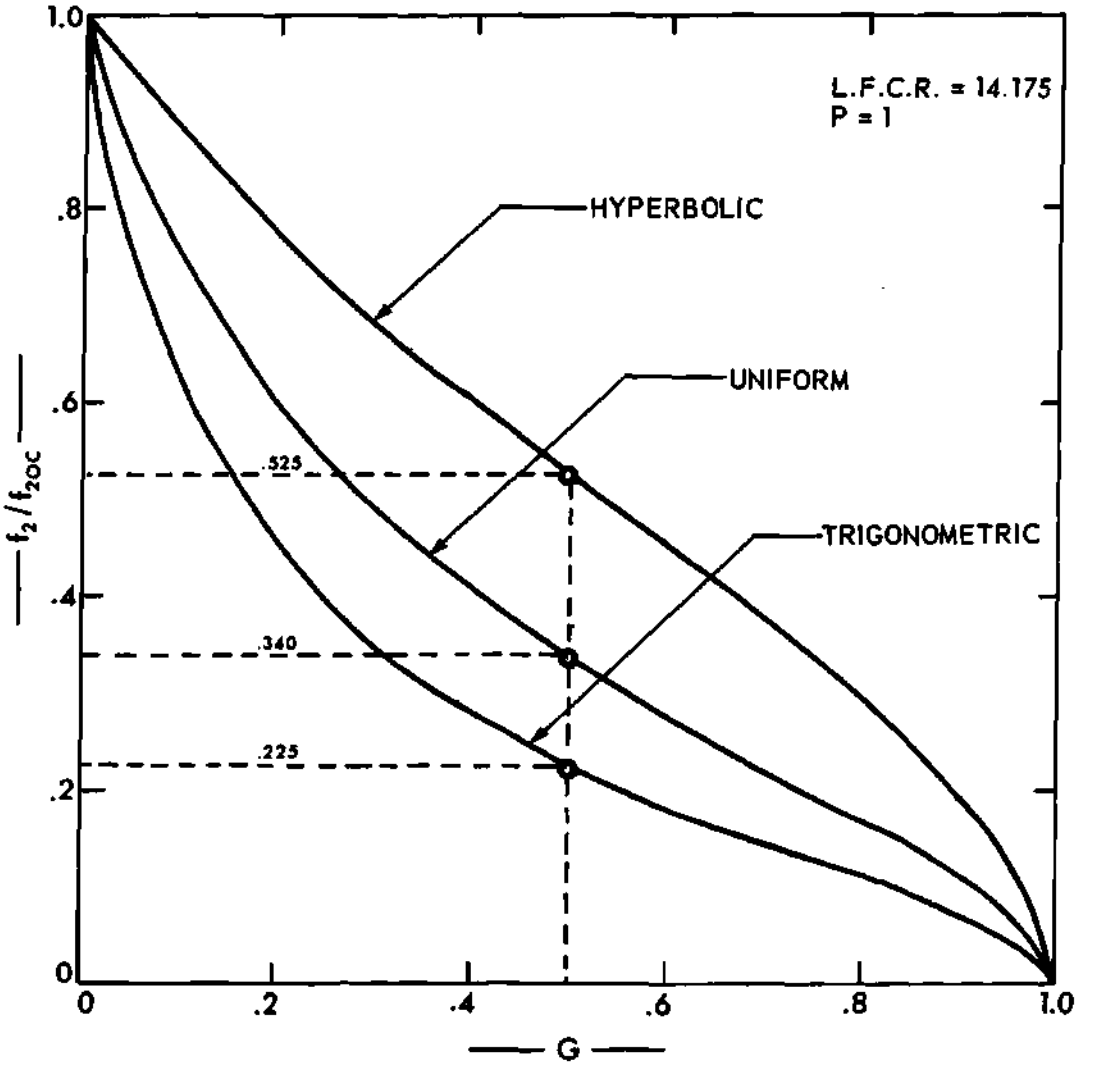

Figure 19. Shift in f_2/f_{2oc} Resulting From Loads With Constant P(P=1) and Variable G for 3 Resembling Lines, L.F.C.R. = 14.175

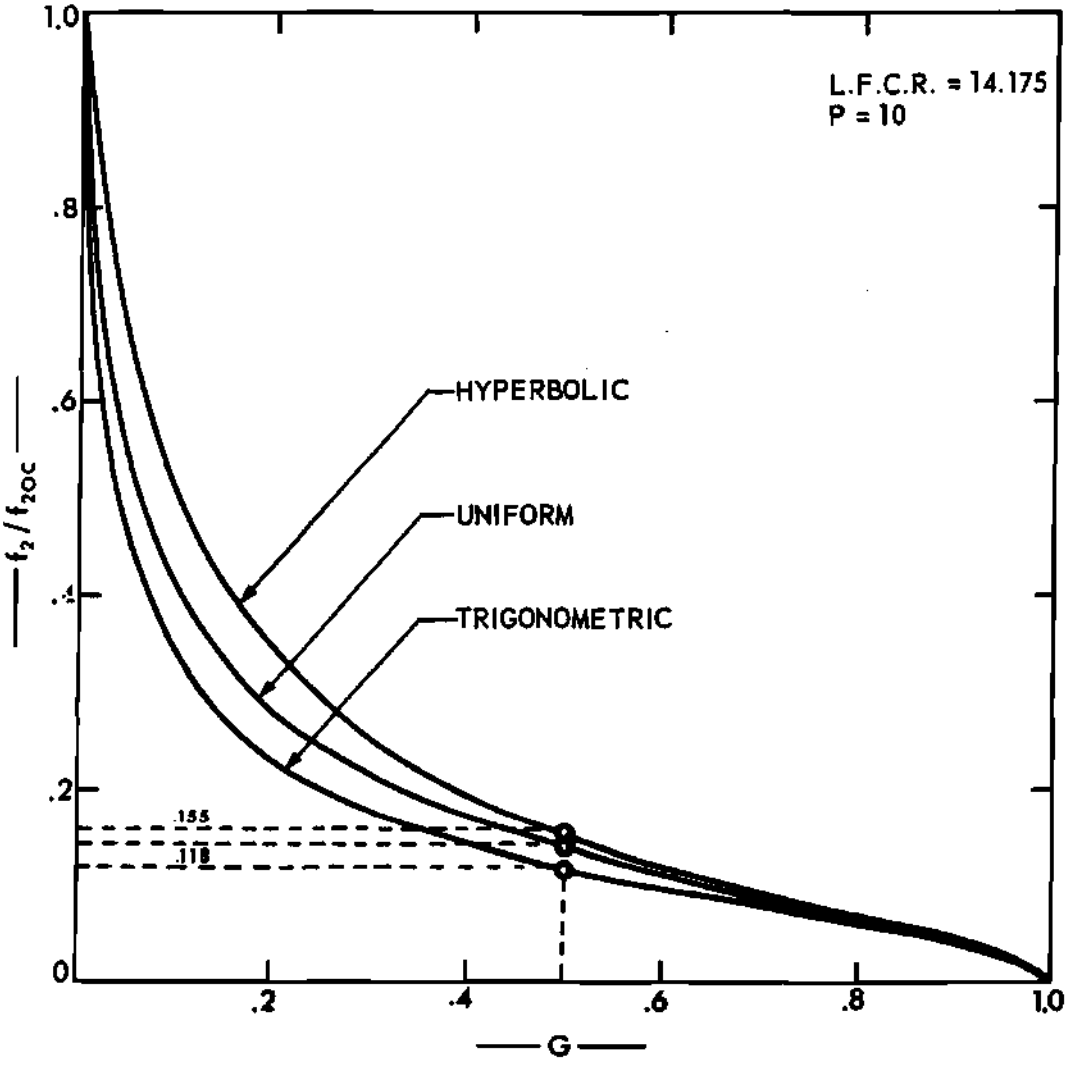

Figure 20. Shift in f_2/f_{2oc} Resulting From Loads With Constant P(P=10) and Variable G for 3 Resembling Lines, L.F.C.R. = 14.175

on these curves represents the voltage-transfer characteristics of a particular network terminated in a specific load. For example, the broken curves of Figure 17 for G = 0.5, P = 10 are represented as the circled points of Figure 20.

A continuous representation of the shift in the curves of Figure 18 as the load capacitance is increased is obtained by holding the normalized load conductance constant and recording the changes in the normalized 30 db attenuation frequencies for each line as the normalized load capacitance is varied. Such a representation for G = 0.5 is illustrated in Figure 21. Essentially this figure is a cross-sectional plot of figures such as 18, 19, and 20 through the vertical G = 0.5 line. The curves of these figures are represented as points on Figure 21. For example, the points corresponding to P = 1 and P = 10, which represent the curves of Figures 19 and 20, are marked for identification. Since in Figure 21 as in Figure 18, the curves for the hyperbolic line are above those representing the uniform and trigonometric lines, the voltage-transfer characteristics of this network, for all practical loads, remained more like its open-circuit characteristics. Thus, these two figures provide theoretical verifications of the predicted performance for these three resembling lines with cut-off ratios of 14.175.

The use of curves like those of Figures 18 and 21 to represent terminated voltage-transfer characteristics makes possible efficient and effective comparisons of the performance of other resembling RC-thin-film networks terminated in all practical loads. Such comparisons of the characteristics of resembling uniform, exponential, trigonometric, and hyperbolic networks with low-frequency-cut-off ratios of 9, 14.176, and

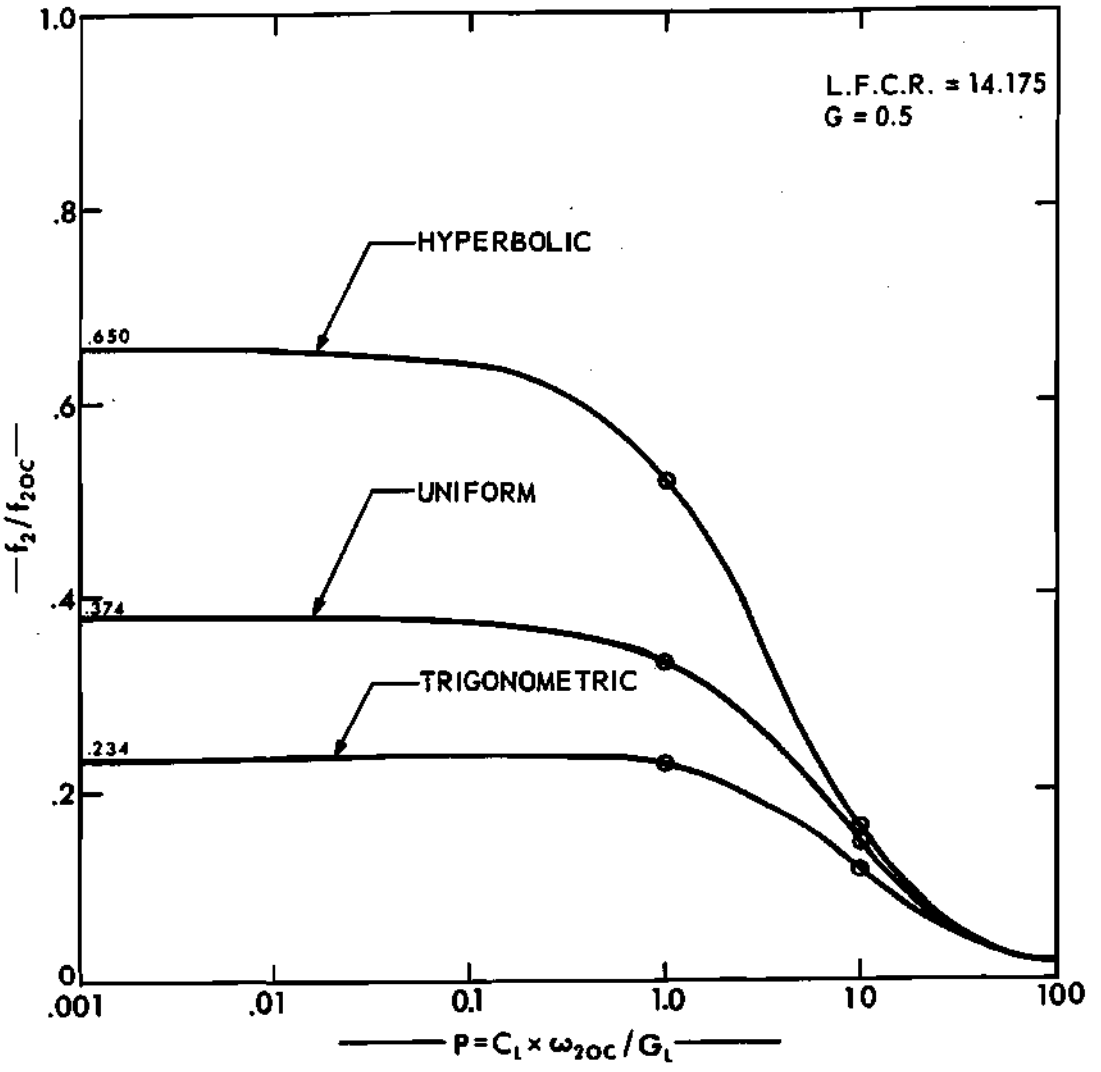

Figure 21. Shift in f_2/f_{2oc} Resulting From Loads with Constant G and Variable P for 3 Resembling Lines, L.F.C.R. = 14.175

20 comprise the majority of both the theoretical and experimental portions of this investigation. The results of the theoretical comparisons are presented throughout the remainder of this chapter.

A representation of the voltage-transfer characteristics of a hyperbolic line ($x_1 = -5.000$, $x_2 = 1.283$), a trigonometric line ($x_1 = 2.400$, $x_2 = 3.128$), and an exponential line ($\alpha\lambda = 3.007$) with low-frequency-cut-off ratios of 9 is presented in Figures 22 and 23. Here again the normalized 30-db attenuation frequency of the hyperbolic line exceeds that of the other two networks for all loads.

Figures 24 and 25 represent the transfer characteristics of a hyperbolic line ($x_1 = -5.000$, $x_2 = 2.176$), a trigonometric line ($x_1 = 0.300$, $x_2 = 2.544$), and an exponential line ($\alpha\lambda = -1.778$) with cut-off ratios of 20. As in the comparisons of networks with low-frequency-cut-off ratios of 9 and 14.175, the voltage-transfer characteristics of the hyperbolic line remain more nearly like the resembling open-circuit curves for all loads. Therefore, the shape and relative location of the curves obtained from the study of these three sets of resembling lines are in agreement with predictions in every instance.

The trigonometric and hyperbolic lines that are used in these investigations are only samples from the infinite number of such lines with cut-off ratios of 9, 14.175, and 20. Therefore, before any general conclusions can be made from the above results, similar studies have to be conducted for other resembling trigonometric and hyperbolic lines. It is decided that a separate investigation of each of these two types of networks will prove to be most effective.

Figure 26 and the top graph of Figure 29 represent the terminated

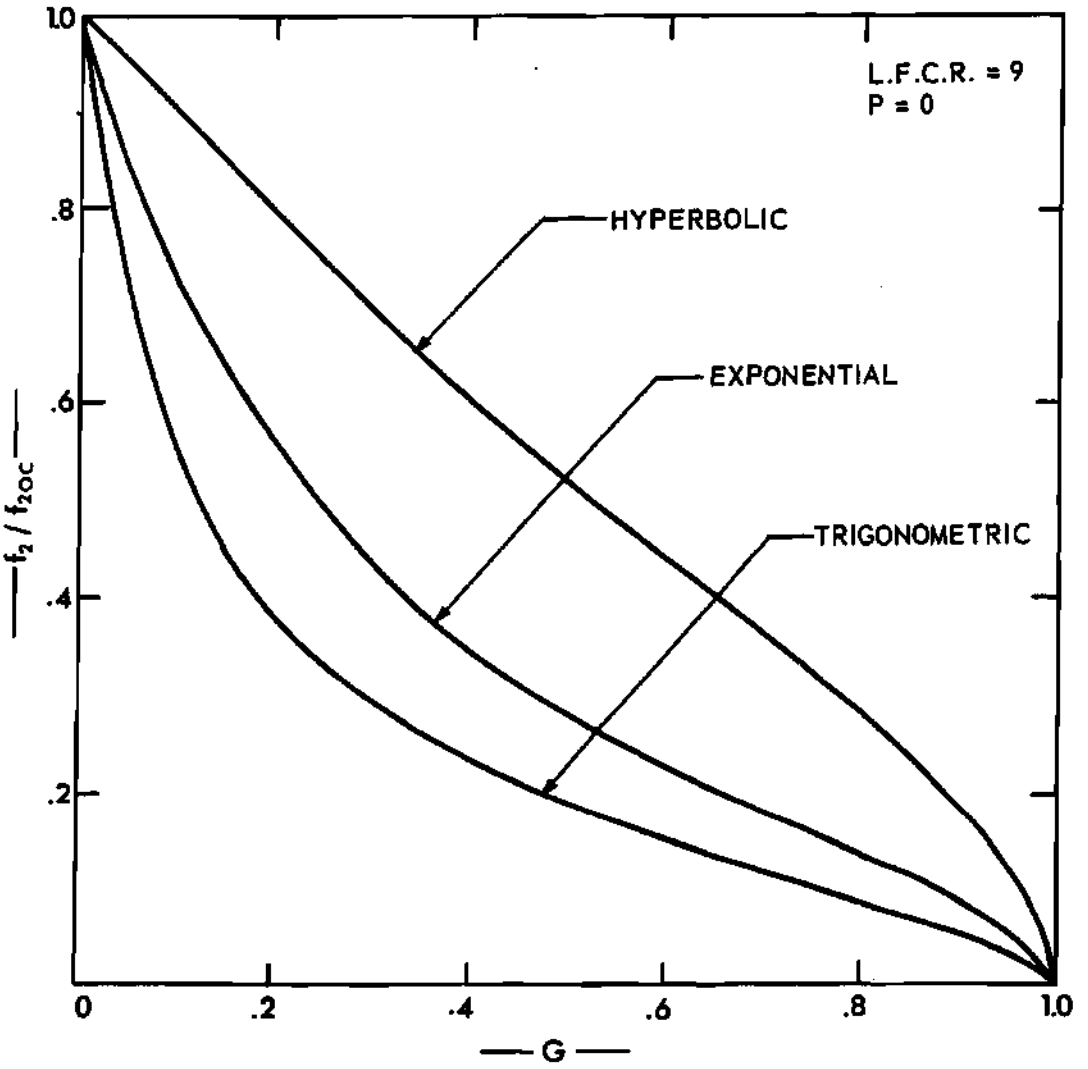

Figure 22. Shift in f_2/f_{2oc} Resulting From Loads with Constant P and Variable G for 3 Resembling Lines, L.F.C.R. = 9

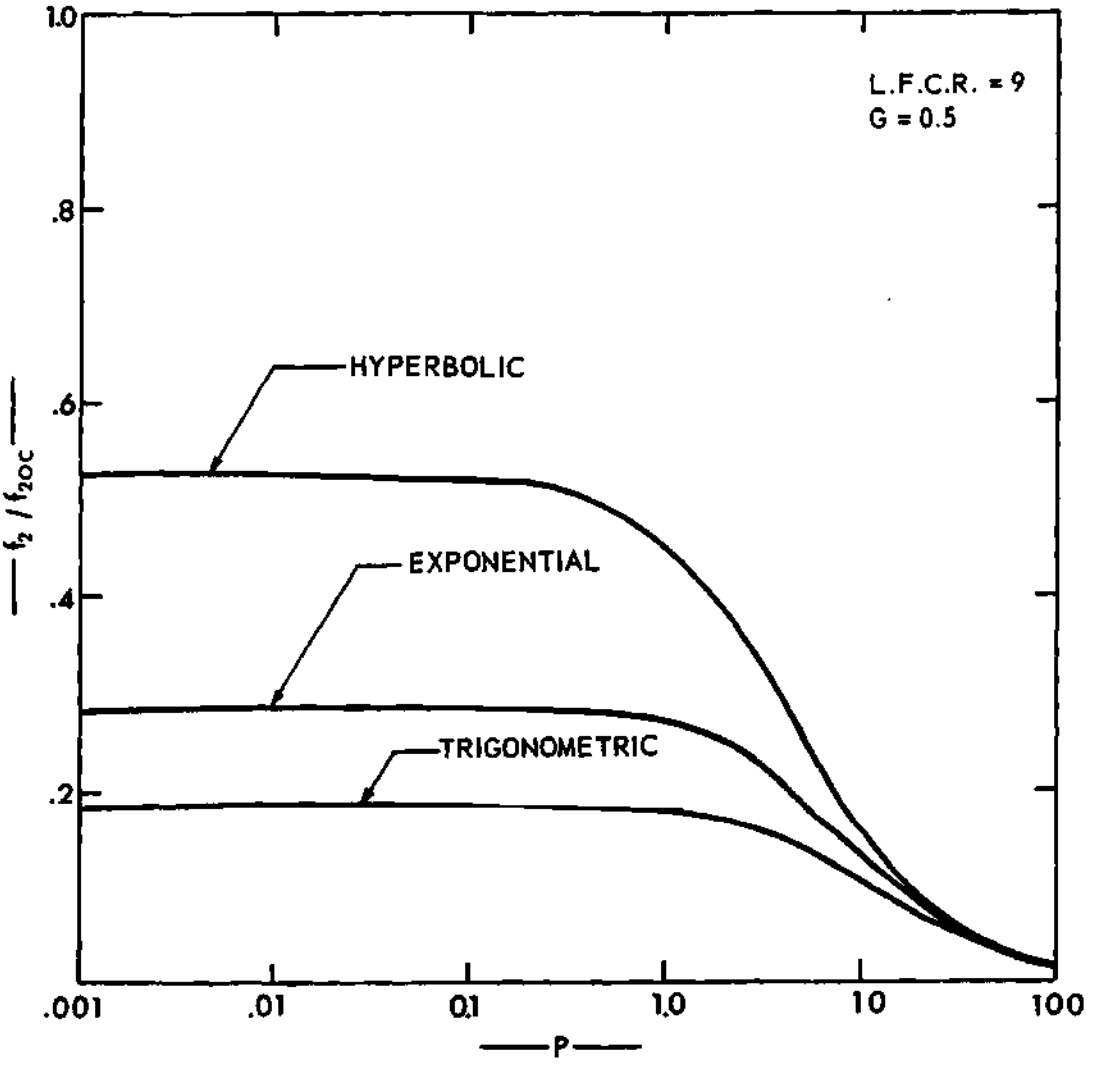

Figure 23. Shift in f_2/f_{2oc} Resulting From Loads with Constant G and Variable P for 3 Resembling Lines, L.F.C.R. = 9

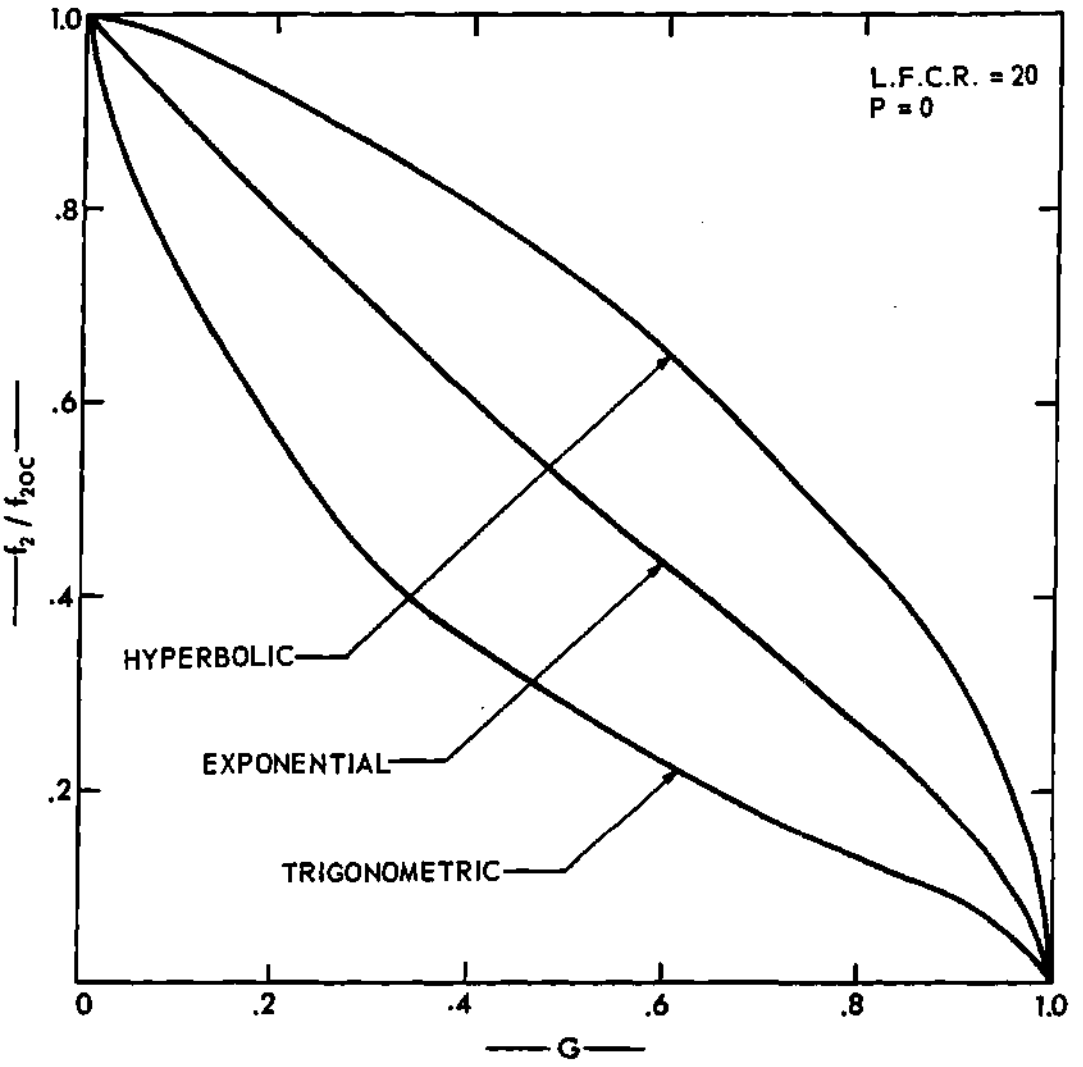

Figure 24. Shift in f_2/f_{2oc} Resulting From Loads With Constant P and Variable G for 3 Resembling Lines, L.F.C.R. = 20

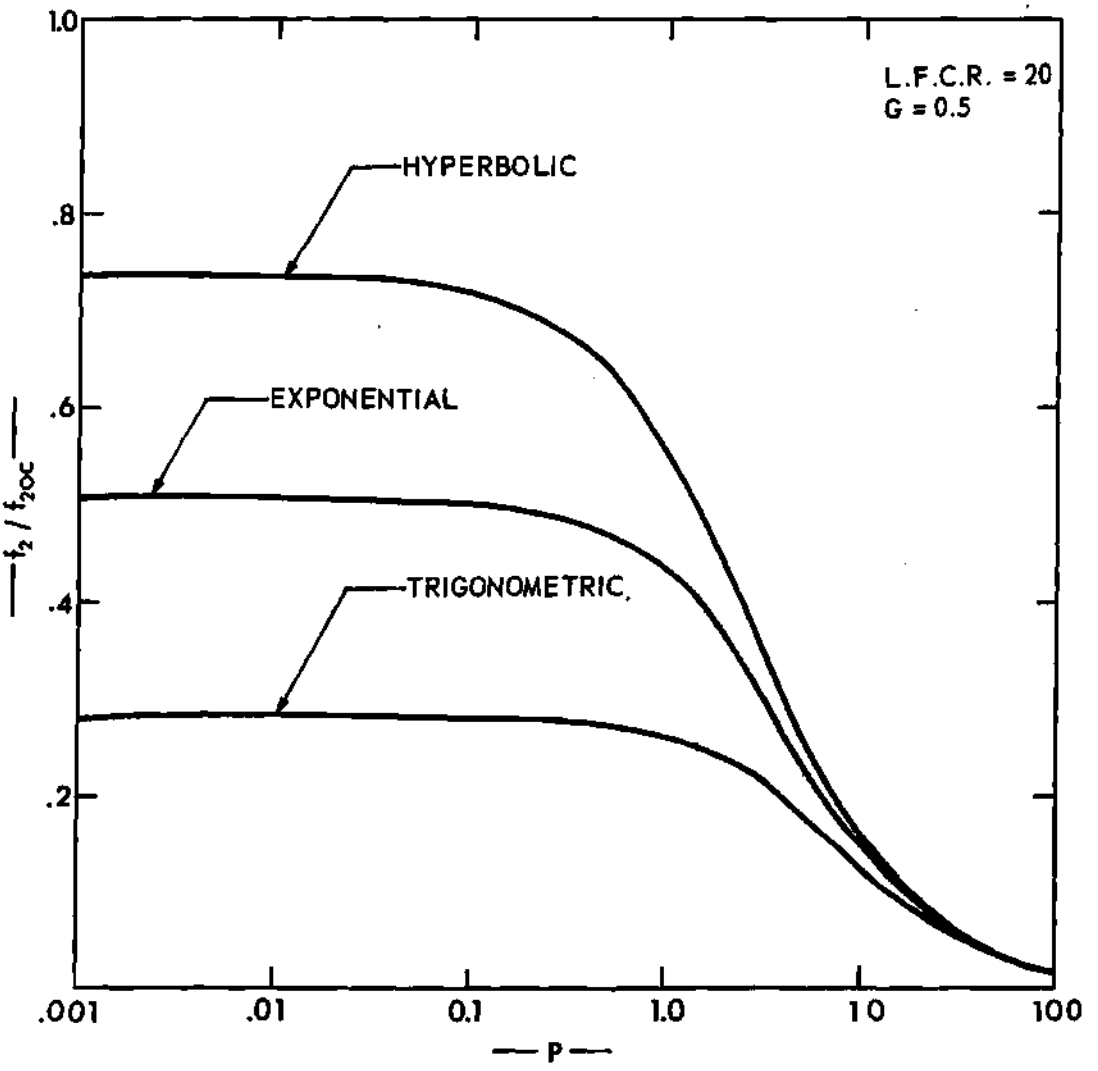

Figure 25. Shift in f_2/f_{2co} Resulting From Loads with Constant G and Variable P for 3 Resembling Lines, L.F.C.R. = 20

voltage-transfer characteristics of two trigonometric lines with cut-off ratios of 9. Line 1 is the same network (L.F.C.R. = 9) that was used in the previous investigation, and line 2 is a trigonometric line with x_1 = 3.00 and x_2 = 3.126. The values of the parameters for each of these networks are marked on the L.F.C.R. = 9 contour of Figure 10. It should be noted that these two networks are representative of two extreme combinations of x_1 and x_2 for trigonometric lines with cut-off ratios of 9. Since there is very little difference in the actual shape of these lines, it is expected that their terminated characteristics will be quite similar. The curves of Figures 26 and 29 confirm this expectation. It is noted, however, that the characteristics of line 2, the network with the larger value of x_1, are less subject to changes due to increased loading.

Figures 27, 28, and 29 similarly represent the terminated characteristics of resembling trigonometric networks with low-frequency-cut-off ratios of 14.175 and 20. In both cases, line 1 is identical with the trigonometric line used in previous comparisons with uniform, exponential, and hyperbolic lines. Line 2 with a low-frequency-cut-off ratio of 14.175 (Figure 27) has the following parameters: x_1 = 1.550, x_2 = 1.592; line 2 with a low-frequency-cut-off ratio of 20 (Figure 28) has the following parameters: x_1 = 0.100, x_2 = 0.253. These parameters are also marked on the contours of Figure 10.

Each of these sets of curves illustrates the effect that parameter changes have on the voltage-transfer characteristics of these trigonometric networks terminated in parallel resistance-capacitance loads. However, before any generalized conclusions can be made from these results to include all trigonometric lines, a study has to be made of resembling lines

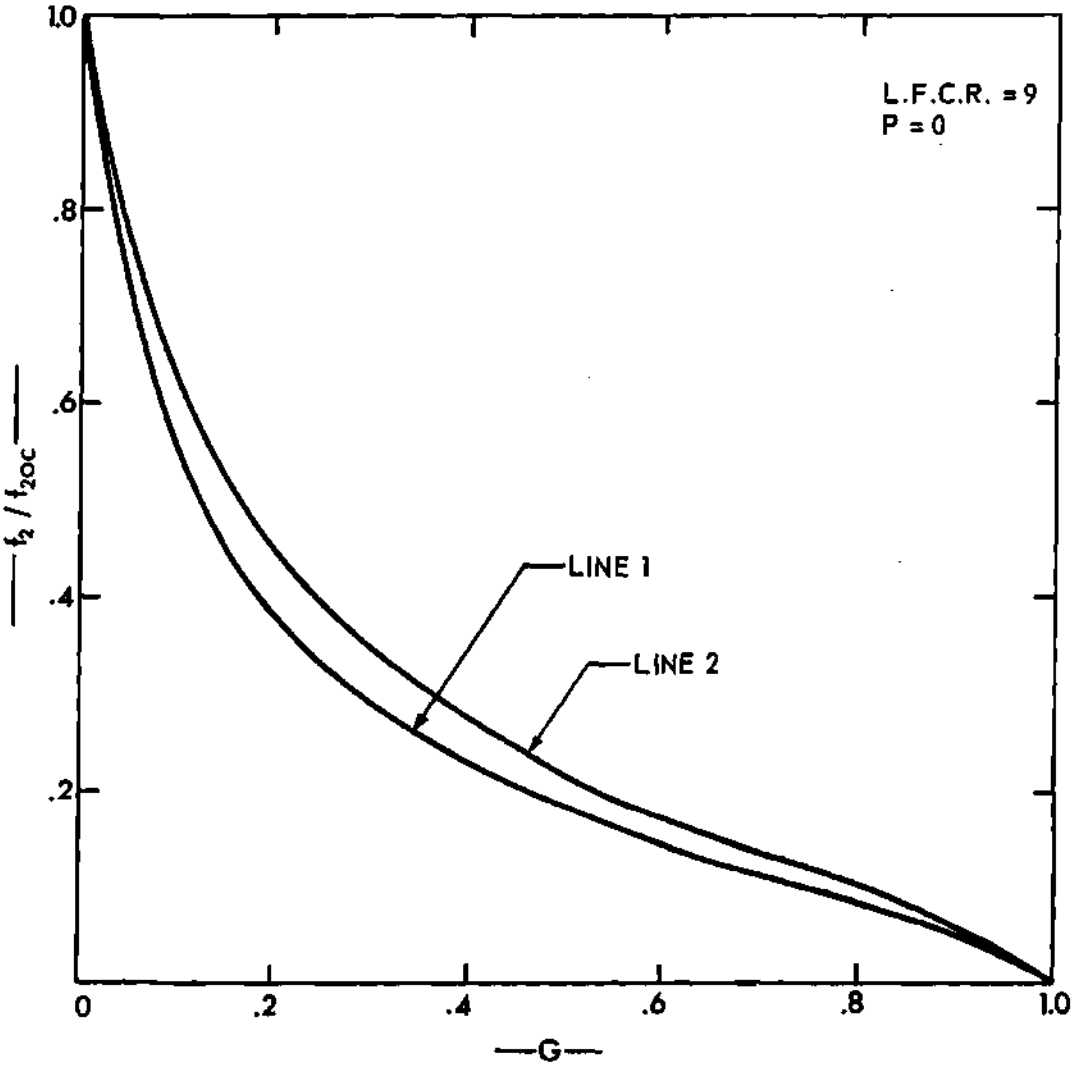

Figure 26. Shift in f_2/f_{2oc} Resulting From Loads with Constant P and Variable G for Two Trigonometric Lines, L.F.C.R. = 9

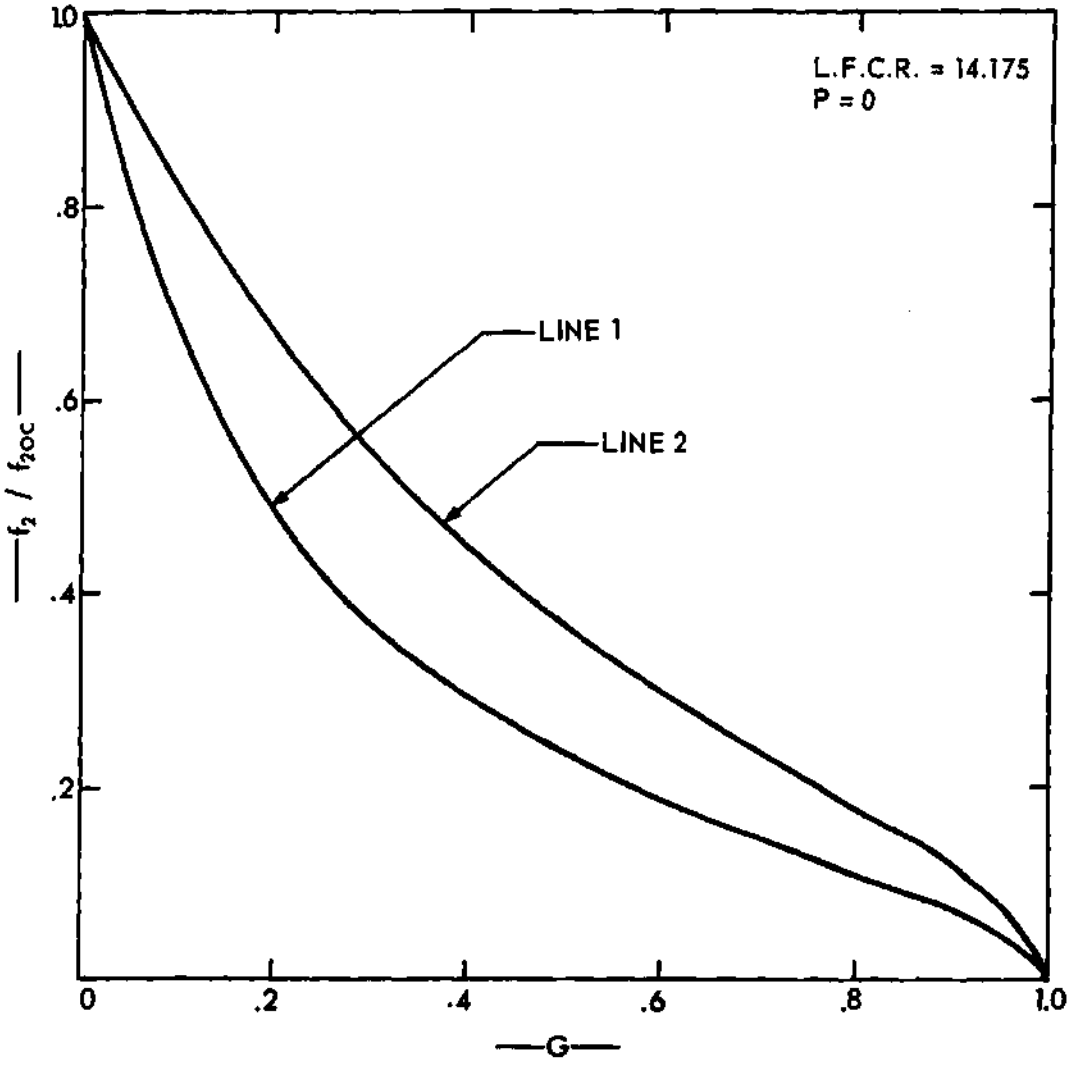

Figure 27. Shift in f_2/f_{2oc} Resulting From Loads with Constant P and Variable G for Two Trigonometric Lines, L.F.C.R. = 14.175

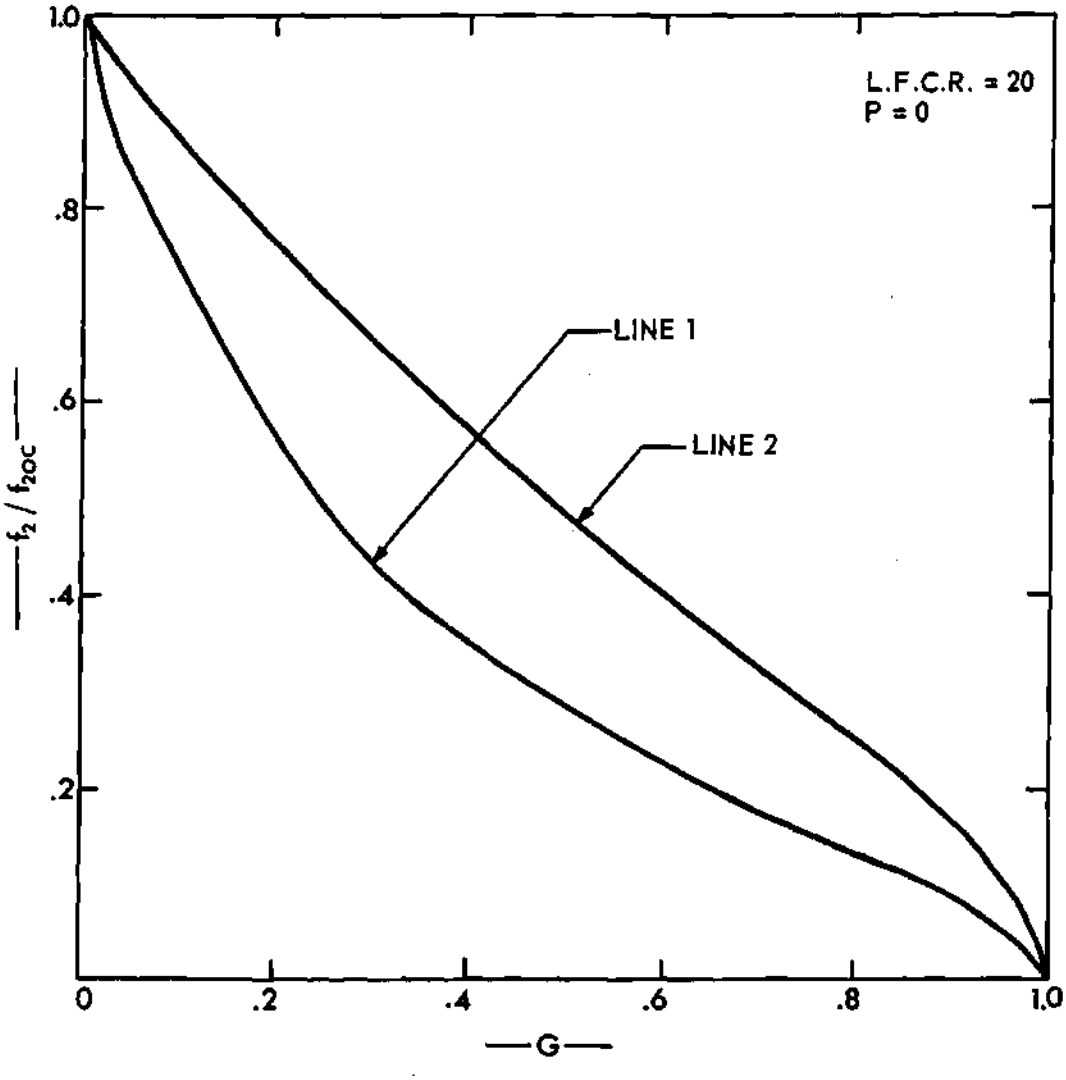

Figure 28. Shift in f_2/f_{2oc} Resulting From Loads with Constant P and Variable G for Two Trigonometric Lines, L.F.C.R. = 20

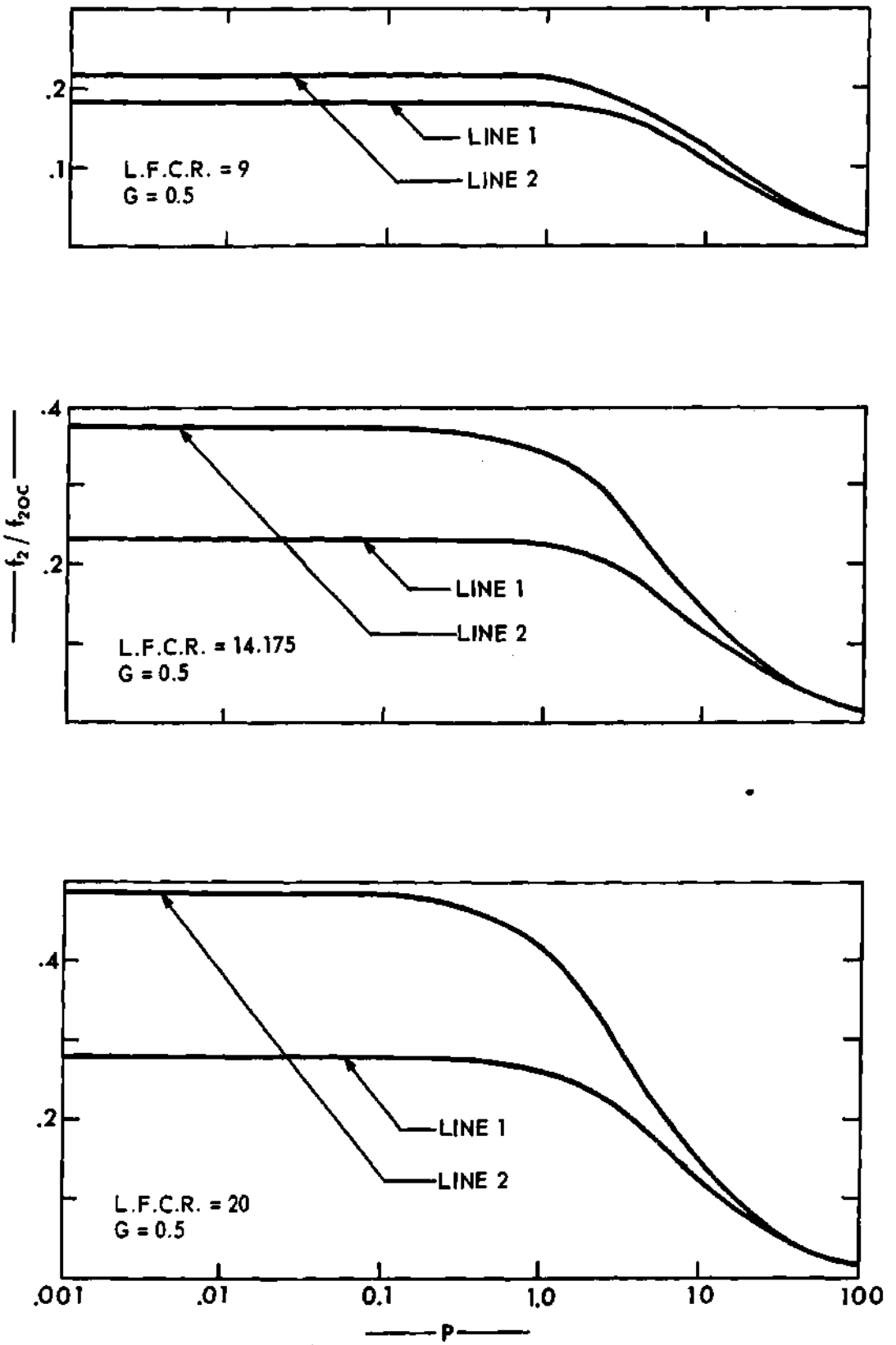

Figure 29. Shift in f_2/f_{2oc} Resulting From Loads with Constant G and Variable P for 3 Groups of Resembling Trigonometric Lines

with other values of x_1 and x_2. Continuous plots of the shift in the voltage-transfer characteristics of resembling trigonometric lines terminated in certain discrete loads versus either x_1 or x_2 prove to be the most effective means of forming a basis for such generalized conclusions. Here again, shifts in transfer characteristics are represented by changes in the normalized 30 db attenuation frequencies.

Figure 30 is such a representation of the transfer characteristics of all practical resembling trigonometric lines with low-frequency-cut-off ratios of 14.175. The curves of this figure are for trigonometric networks terminated in the following pure resistive loads: G = 0.2, G = 0.5, G = 0.8. Each point on these curves represents the terminated voltage-transfer characteristics of a specific trigonometric lines with a cut-off ratio of 14.175. Points on each of the three curves that have the same value of x_1 represent identical networks. The corresponding values of x_2 can be determined from the L.F.C.R. = 14.175 contour of Figure 10. A shift in the normalized 30 db attenuation frequency of a specific network resulting from pure resistive loading is evident in this figure as a shift from one curve to another. However, more important here is the shift in this 30 db frequency as x_1 is varied while holding the load constant. For these three representative values of load conductance, the voltage-transfer characteristics of networks with smaller values of x_1 are shifted further away from the resembling open-circuit characteristics.

Similar curves representing the characteristics of the same lines terminated in certain discrete parallel resistance capacitance loads are depicted in Figure 31. Here again, for each termination the transfer characteristics of networks with larger values of x_1 tend to remain closer

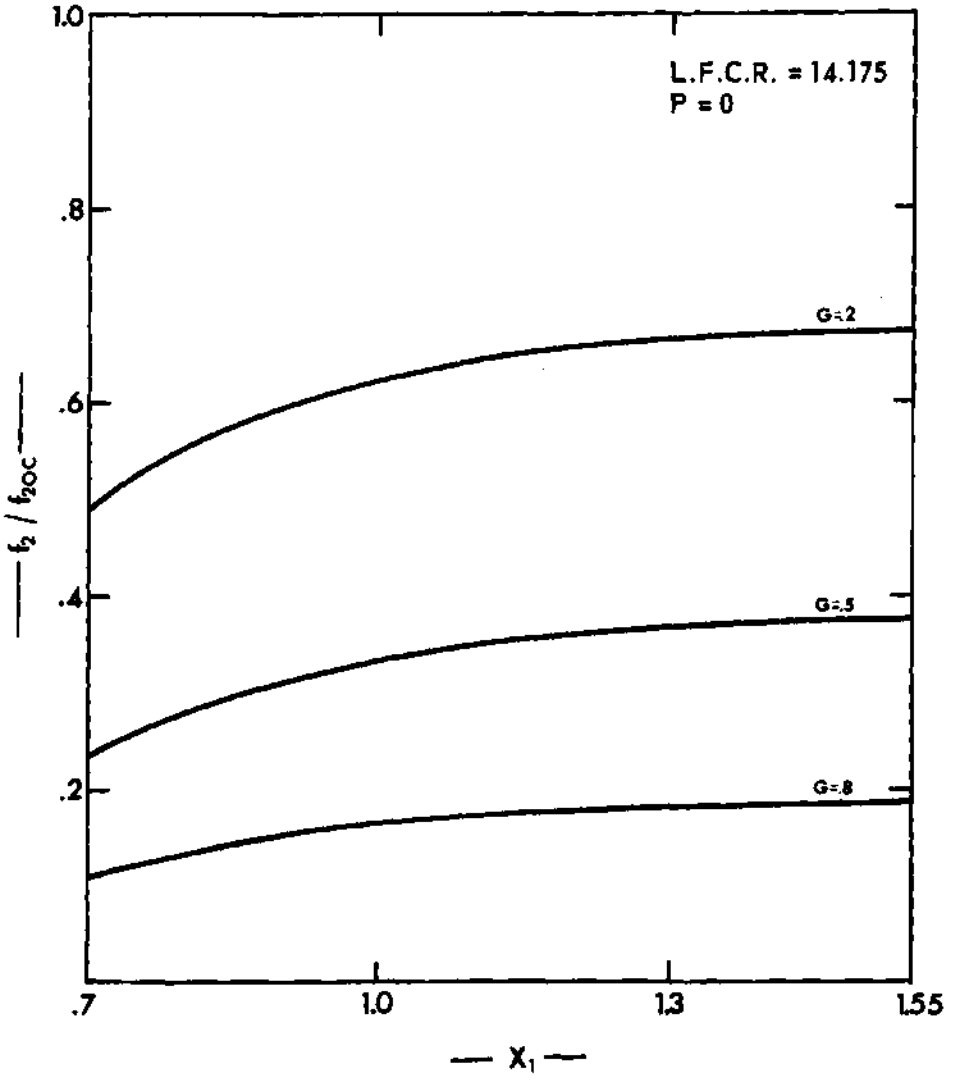

Figure 30. Shift in f_2/f_{2oc} for Constant Loads as x_1 Is Varied for Resembling Trigonometric Lines, L.F.C.R. = 14.175

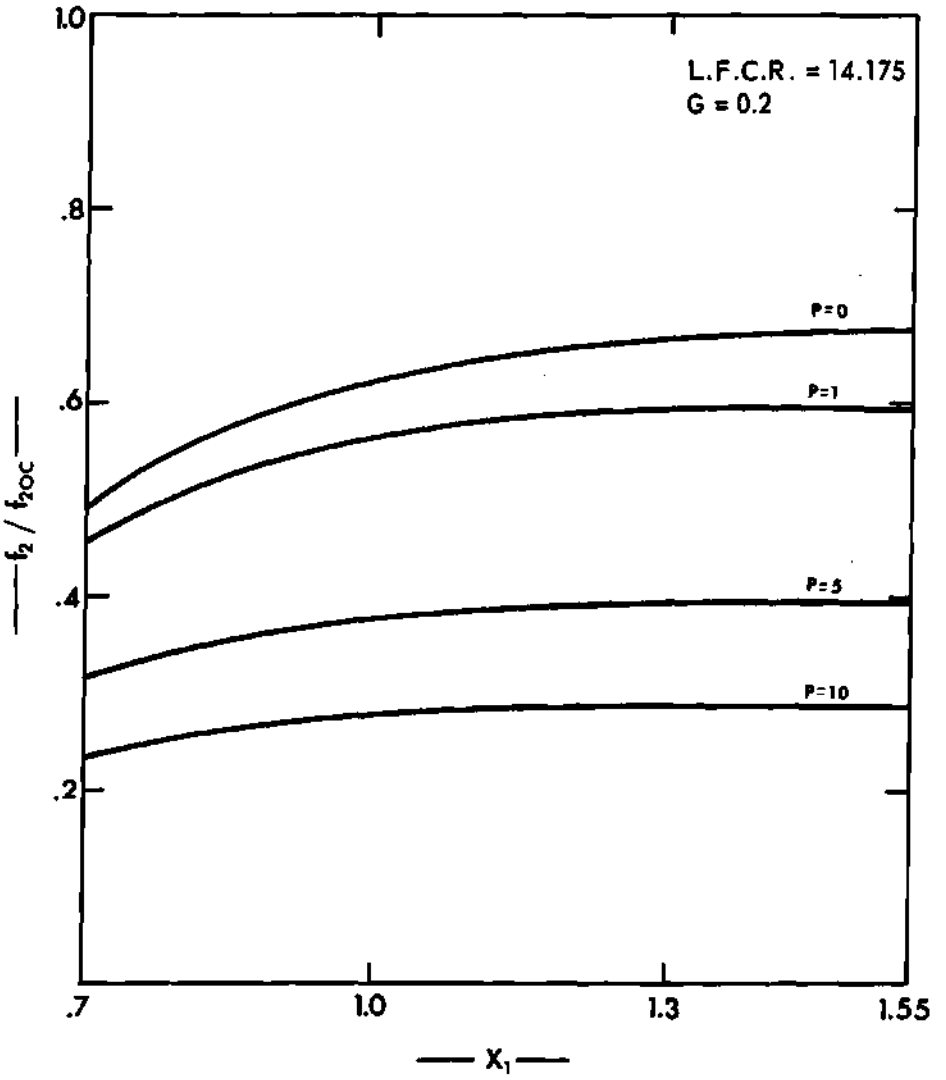

Figure 31. Shift in f_2/f_{2oc} for Constant Loads as x_1 Is Varied for Resembling Trigonometric Lines, L.F.C.R. = 14.175

to the resembling open-circuit curves. It is therefore concluded from these two sets of curves that the voltage-transfer characteristics of trigonometric lines with cut-off ratios of 14.175 are less subject to changes due to parallel resistance capacitance terminations when the values of x_1 are large.

Figures 32 and 33 depict similar curves for trigonometric lines with low-frequency-cut-off ratios of 9 and 20 respectively. Since the L.F.C.R. = 20 contour of Figure 10 is double-valued with respect to x_1, the normalized 30 db frequency in Figure 33 is plotted as a function of x_2. The corresponding values of x_1 and x_2 for the networks represented in these two figures can be determined from these contours.

Although the normalized load conductances and capacitances in Figures 32 and 33 are limited to several discrete values, these values prove to be representative of all loads. An examination of the curves in these figures reveals that the voltage-transfer characteristics for trigonometric lines with cut-off ratios of 9 remain closer to their resembling open-circuit curves for larger values of x_1, and that for trigonometric lines with cut-off ratios of 20, their transfer characteristics are shifted less for smaller values of x_2. From a critical study of the curves of Figures 30, 31, 32, and 33 and the contours of Figure 10, the following important conclusions concerning the effects of parameter changes on the terminated performance of resembling trigonometric lines are established: the voltage-transfer characteristics of resembling trigonometric lines with low-frequency-cut-off ratios less than or equal to 14.175 are less susceptible to changes resulting from parallel resistance-capacitance terminations when the value of x_1 is as large as possible;

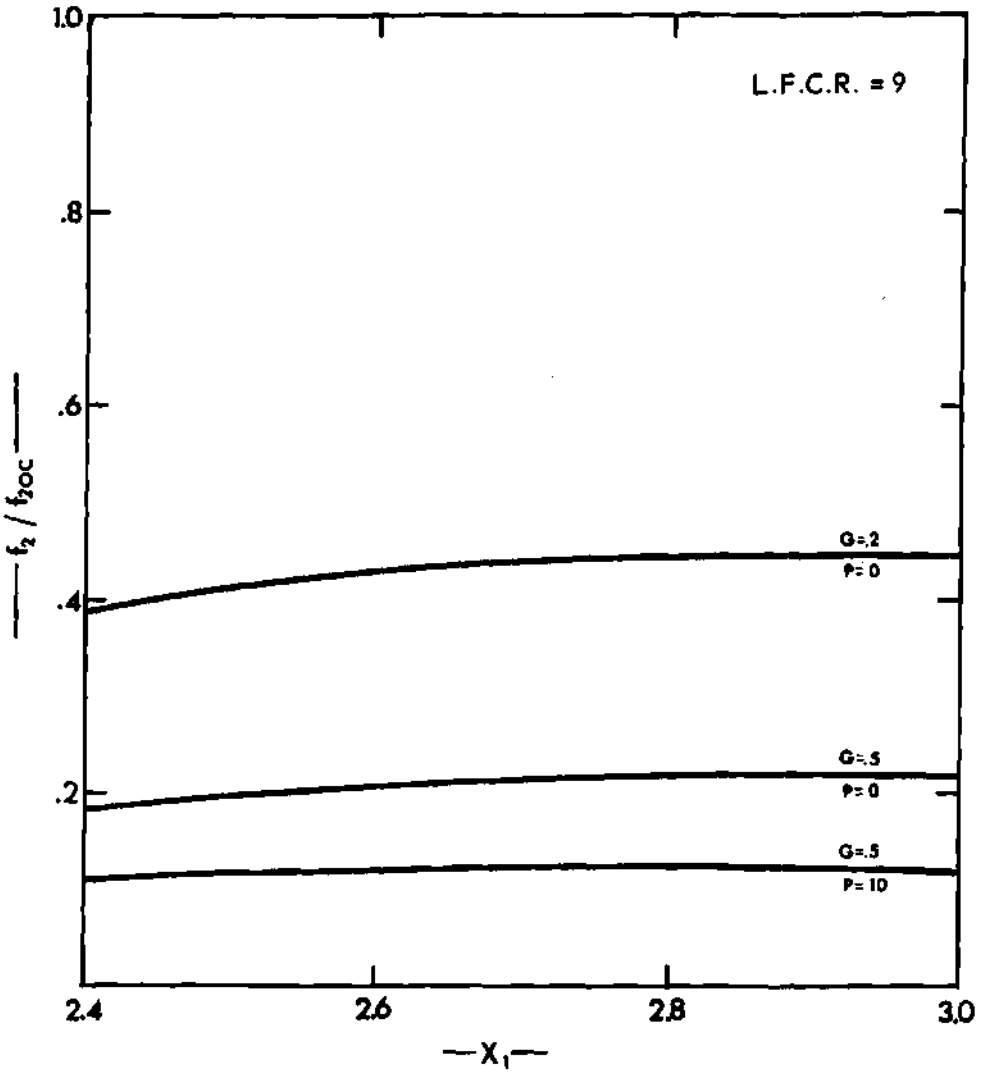

Figure 32. Shift in f_2/f_{2oc} for Constant Loads as x_1 Is Varied for Resembling Trigonometric Lines, L.F.C.R. = 9

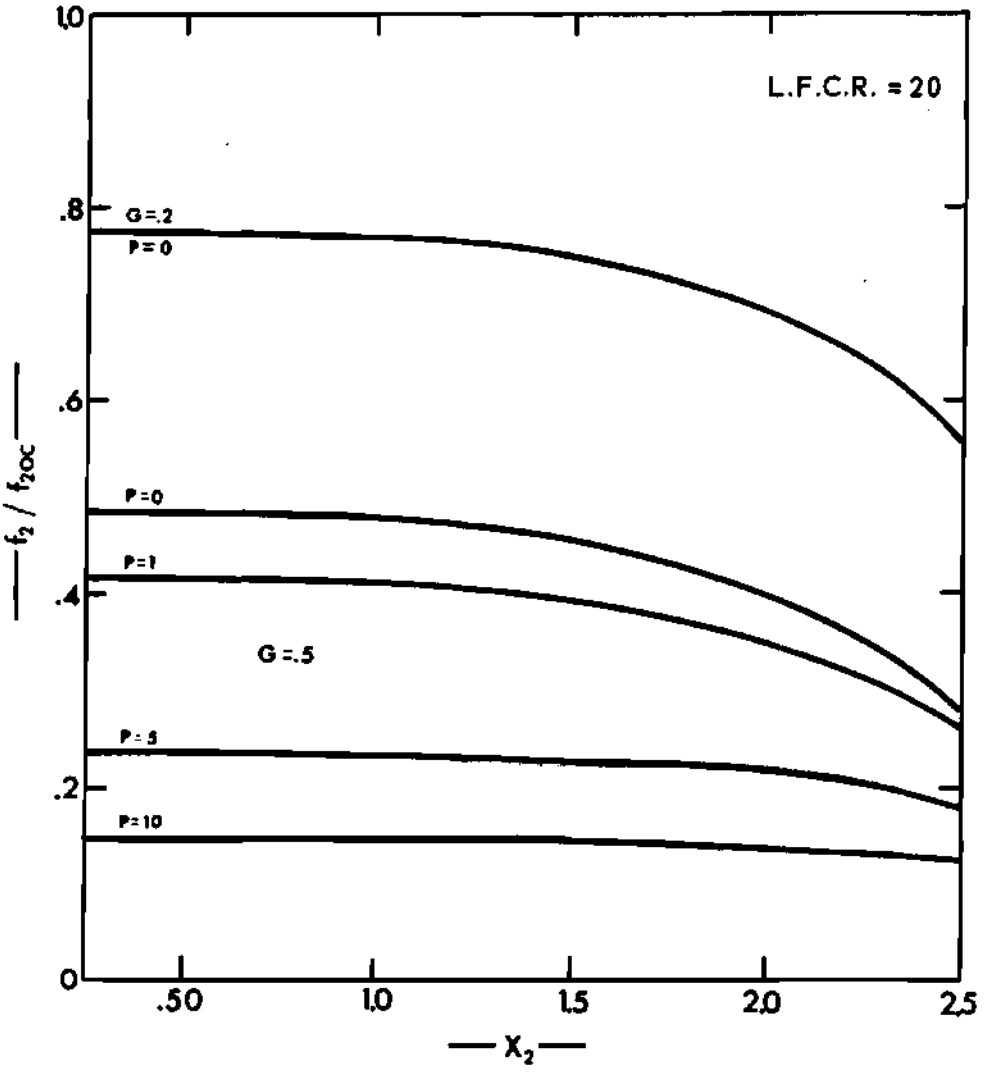

Figure 33. Shift in f_2/f_{2oc} for Constant Loads as x_2 Is Varied for Resembling Trigonometric Lines, L.F.C.R. = 20

the voltage-transfer characteristics of resembling trigonometric lines with low-frequency-cut-off ratios greater than 14.175 are less susceptible to changes resulting from parallel resistance-capacitance terminations when the values of x_2 are as large as possible. Also, for very large terminating impedances, changes in the values of x_1 and x_2 have very little effect on the corresponding voltage-transfer characteristics.

The study of the effects of parameter changes on the terminated voltage-transfer characteristics of resembling hyperbolic lines parallels the corresponding study of resembling trigonometric lines. Here again, the normalized 30-db-attenuation frequency f_2/f_{2oc} is used as an indicator of the relative position of the voltage-transfer characteristics for each different termination.

Figures 34 and 35, 36 and 37, and 38 and 39 represent the characteristics of two resembling hyperbolic lines with low-frequency-cut-off ratios of 9, 14.176, and 20 respectively. In each figure, the network designated line 1 is identical with the hyperbolic line which was compared in previous studies with trigonometric and uniform or exponential lines with the same cut-off ratios. The values of x_1 and x_2 for these networks and for the networks depicted as line 2 are tabulated in Table 2.

Table 2. Values of x_1 and x_2 For Three Pairs of Resembling Hyperbolic Lines

Figures	L.F.C.R.	Line 1		Line 2	
		x_1	x_2	x_1	x_2
34 and 35	9.000	-5.000	1.238	-2.100	0
36 and 37	14.176	-5.000	1.784	-0.100	0.0998
38 and 39	20.000	-5.000	2.176	0	1.462

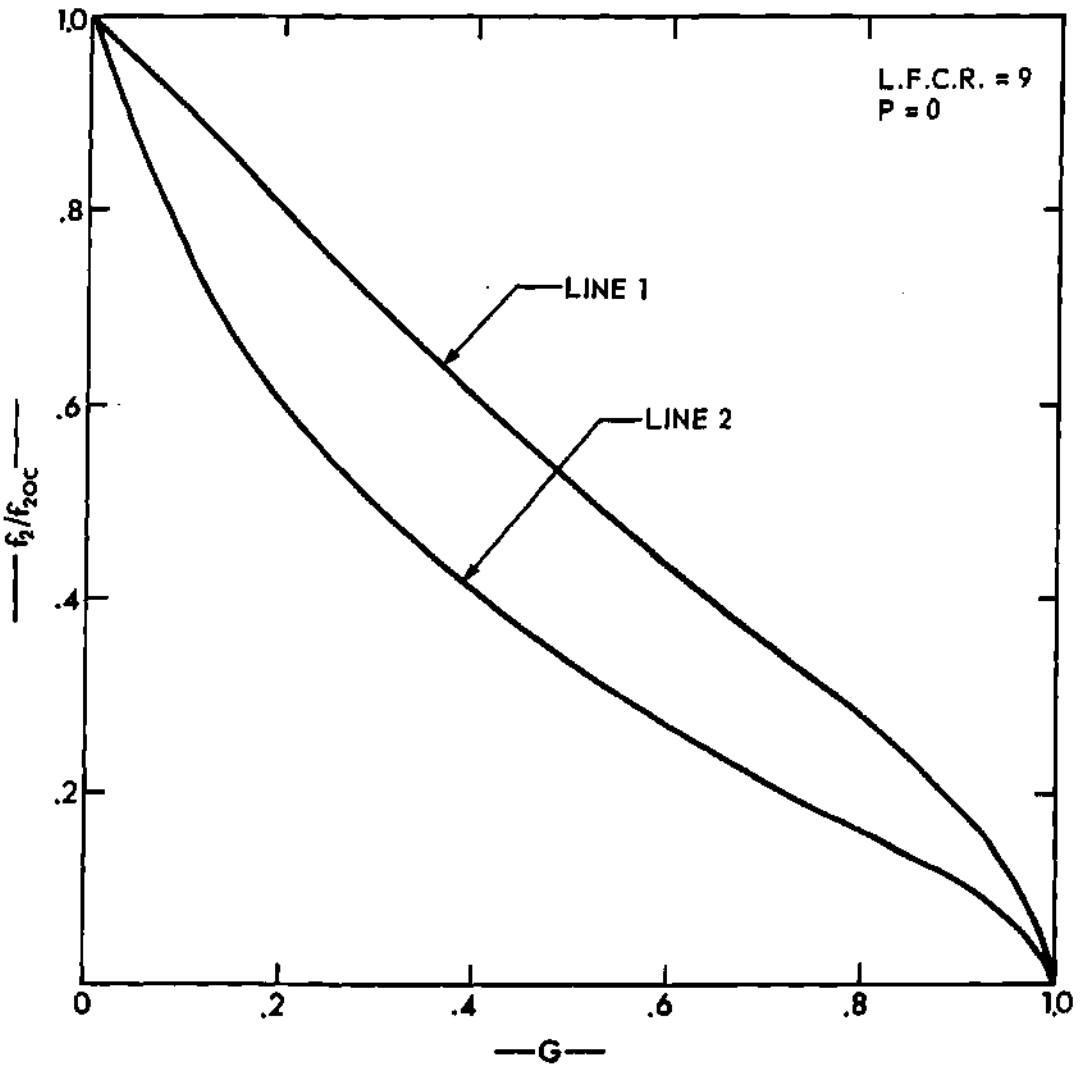

Figure 34. Shift in f_2/f_{2oc} Resulting From Loads with Constant P and Variable G for Two Hyperbolic Lines, L.F.C.R. = 9

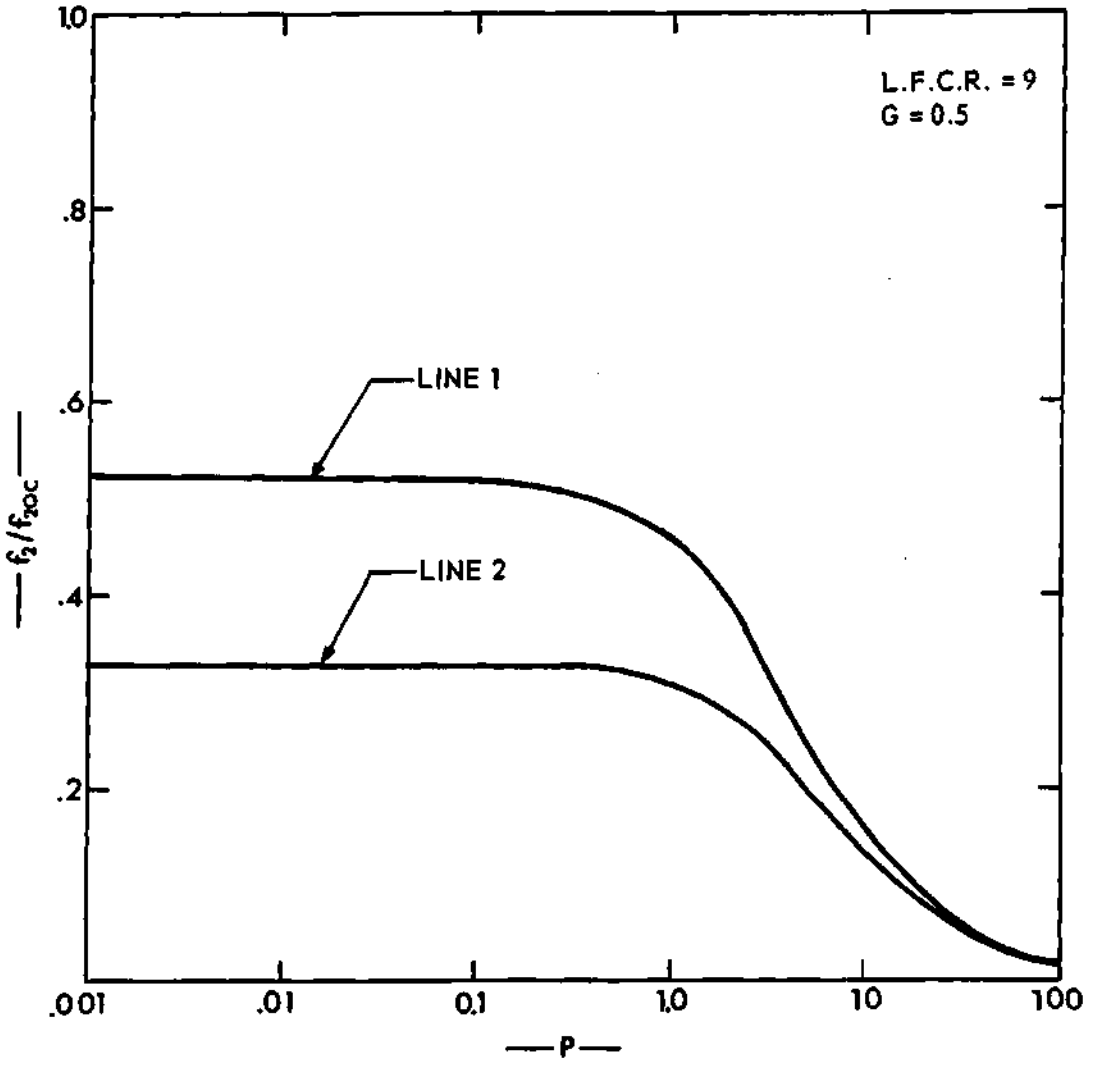

Figure 35. Shift in f_2/f_{2oc} Resulting From Loads with Constant P and Variable P for Two Hyperbolic Lines, L.F.C.R. = 9

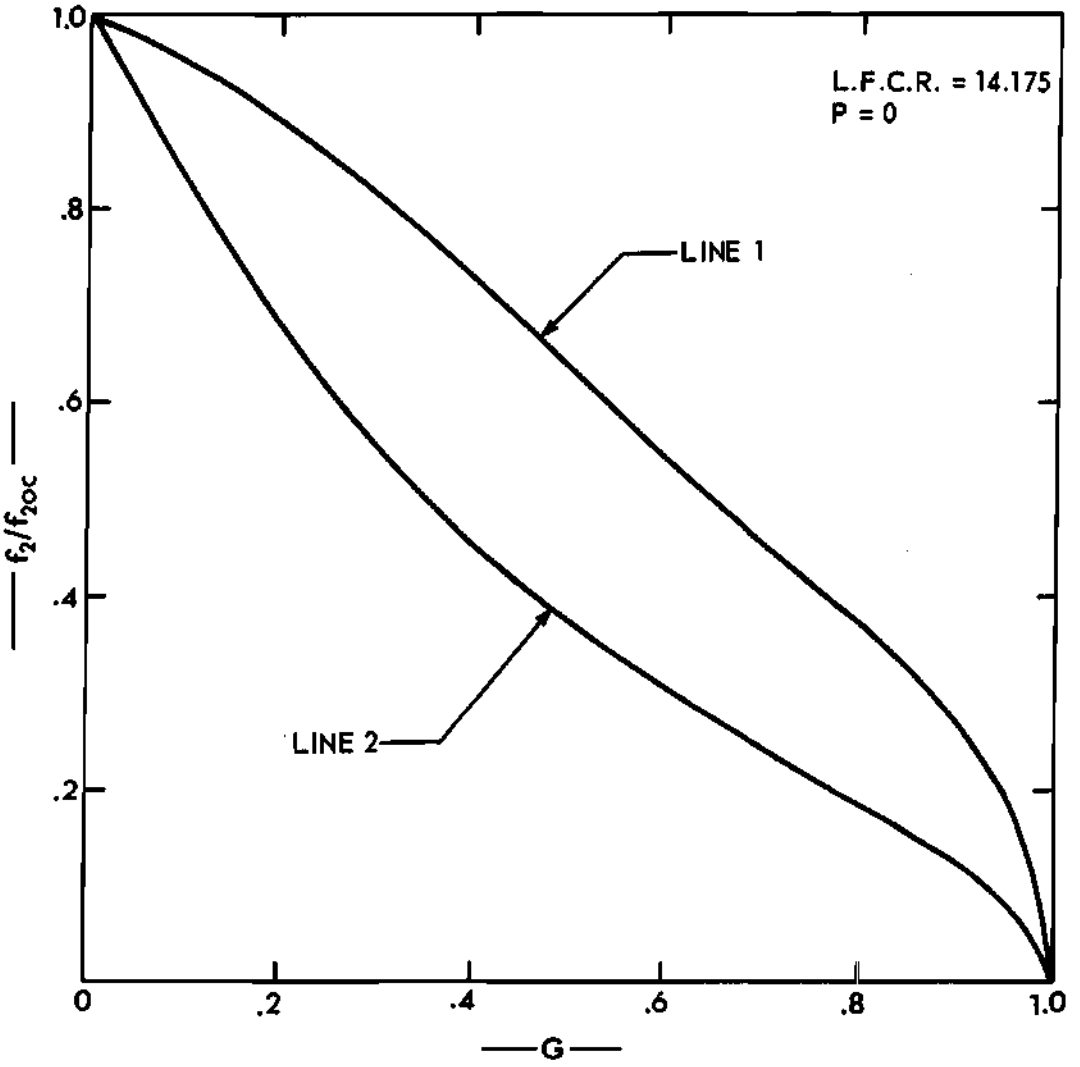

Figure 36. Shift in f_2/f_{2oc} Resulting From Loads with Constant P and Variable G for Two Hyperbolic Lines, L.F.C.R. = 14.175

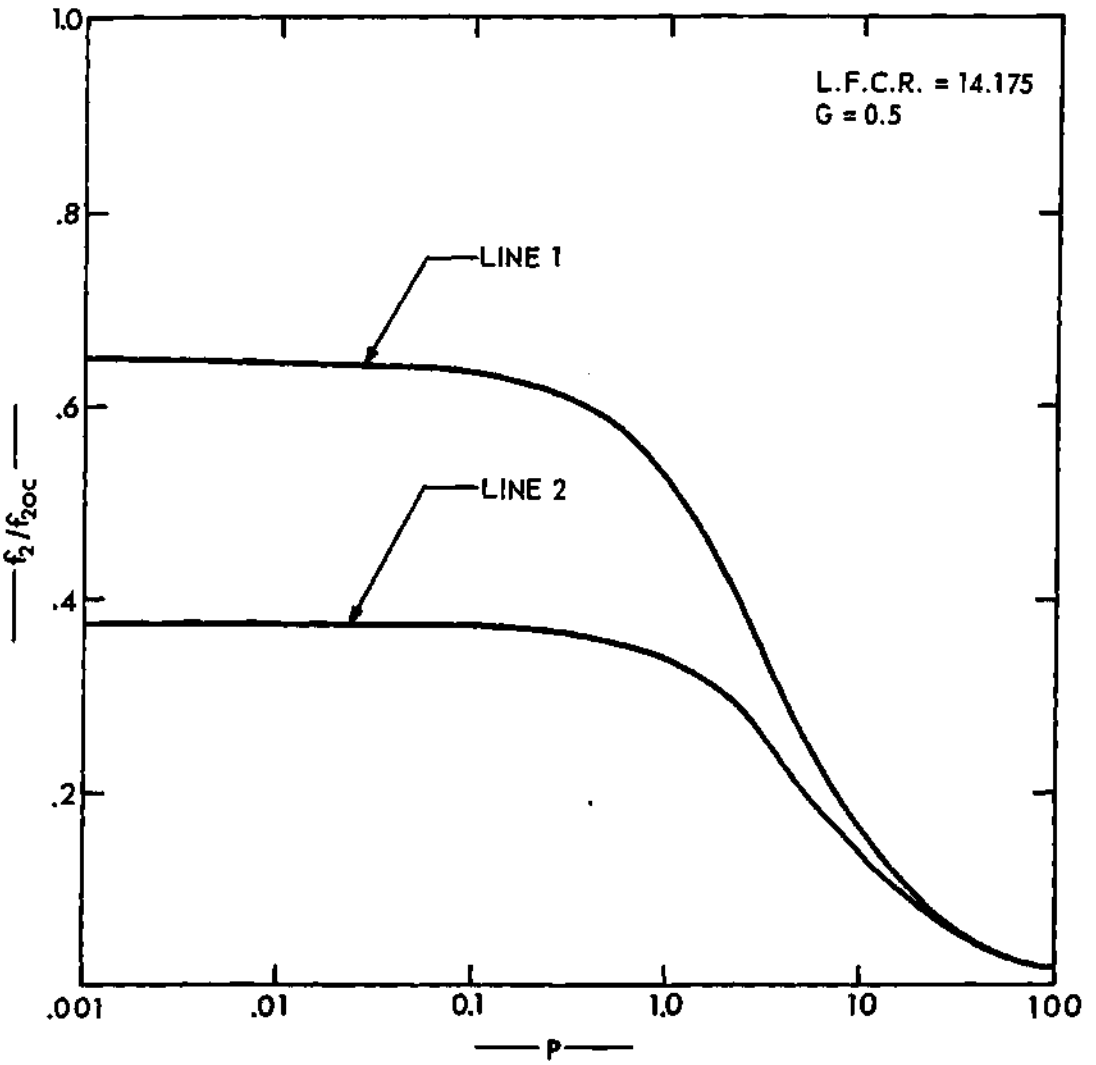

Figure 37. Shift in f_2/f_{2oc} Resulting From Loads With Constant G and Variable P for Two Hyperbolic Lines, L.F.C.R. = 14.175

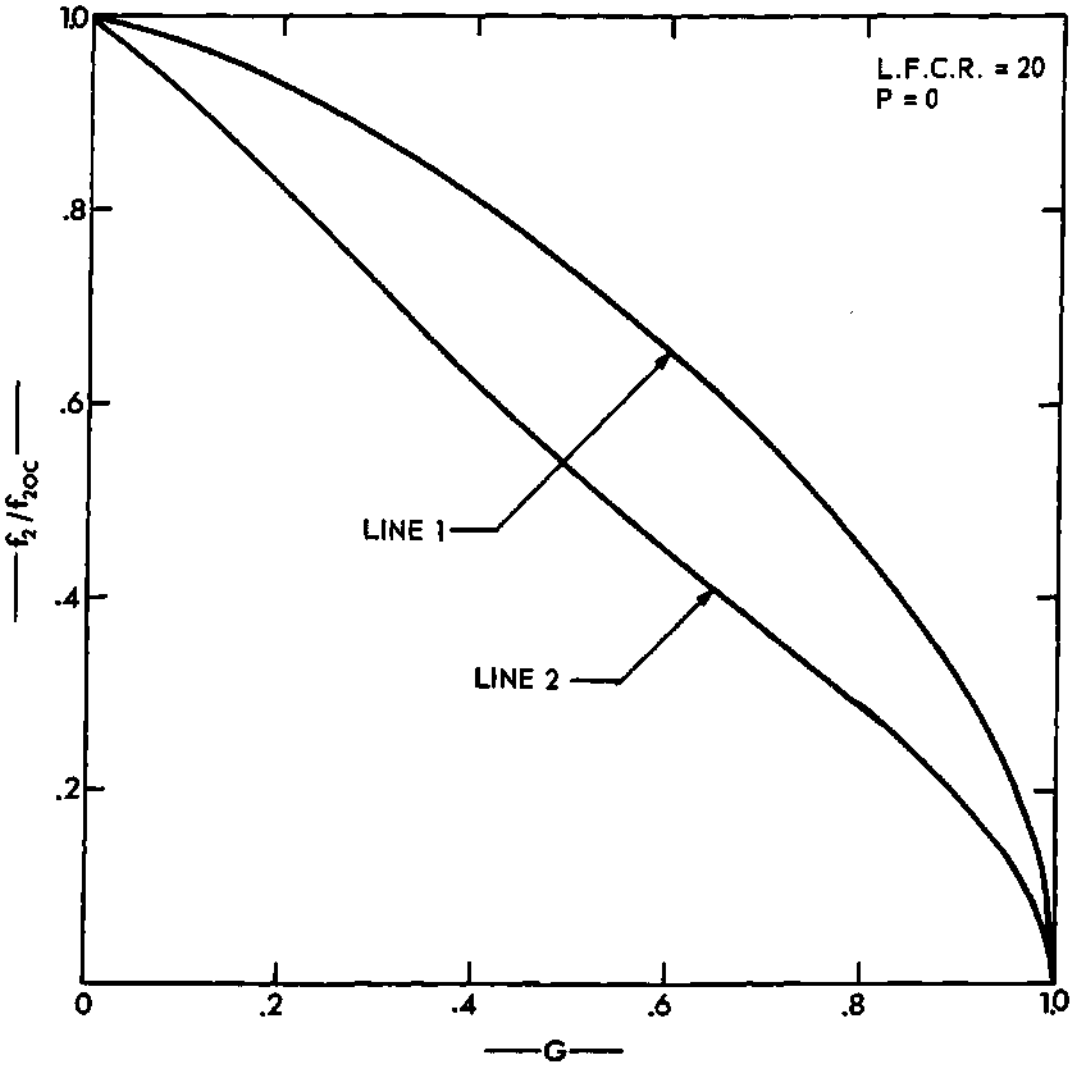

Figure 38. Shift in f_2/f_{2oc} Resulting From Loads with Constant P and Variable G for Two Hyperbolic Lines, L.F.C.R. = 20

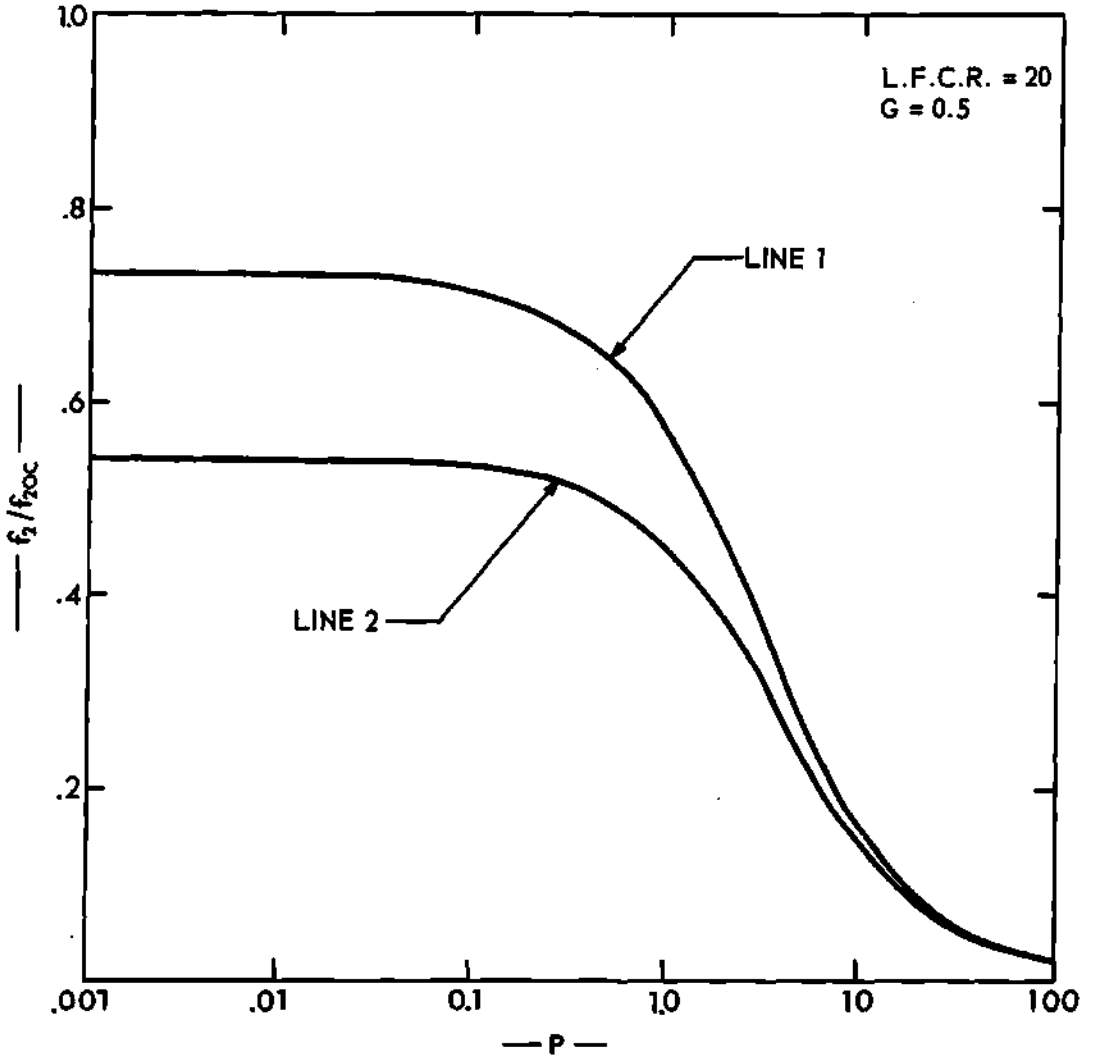

Figure 39. Shift in f_2/f_{2oc} Resulting From Loads with Constant G and Variable P for Two Hyperbolic Lines, L.F.C.R. = 20

The parameters in Table 2 are marked on the contours of Figure 11 and in each case the values of x_1 and x_2 representing line 1 and line 2 lie at opposite extremes of these contours.

In each figure the curves representing the voltage-transfer characteristics of line 1 lie above those of the curves for line 2. Since in every case the value of x_1 for line 1 is larger in the negative direction than the corresponding value of x_1 for line 2, these curves tend to indicate that the transfer characteristics of resembling hyperbolic lines with large negative values of x_1 are less subject to load changes.

Figures 40 and 41 verify this conclusion for all hyperbolic lines with cut-off ratios of 14.175. The curves of Figure 40 represent the characteristics of these networks terminated in three specific pure resistive loads, and the curves of Figure 41 are representative of the characteristics of the same networks terminated in several discrete parallel resistance-capacitance loads. Here again, each point on these curves represents the voltage-transfer characteristics of a specific network, designated by the value of x_1, terminated in a specific load. The corresponding value of x_2 for each of these networks can be determined from the contours of Figure 11.

Figures 42 and 43 represent the terminated voltage-transfer characteristics of all practical hyperbolic lines with cut-off ratios of 9 and 20 respectively. Again, both cases illustrate that networks with larger negative values of x_1 have terminated characteristics which are less subject to load variations.

From a critical study of the curves of Figures 40, 41, 42, and 43,

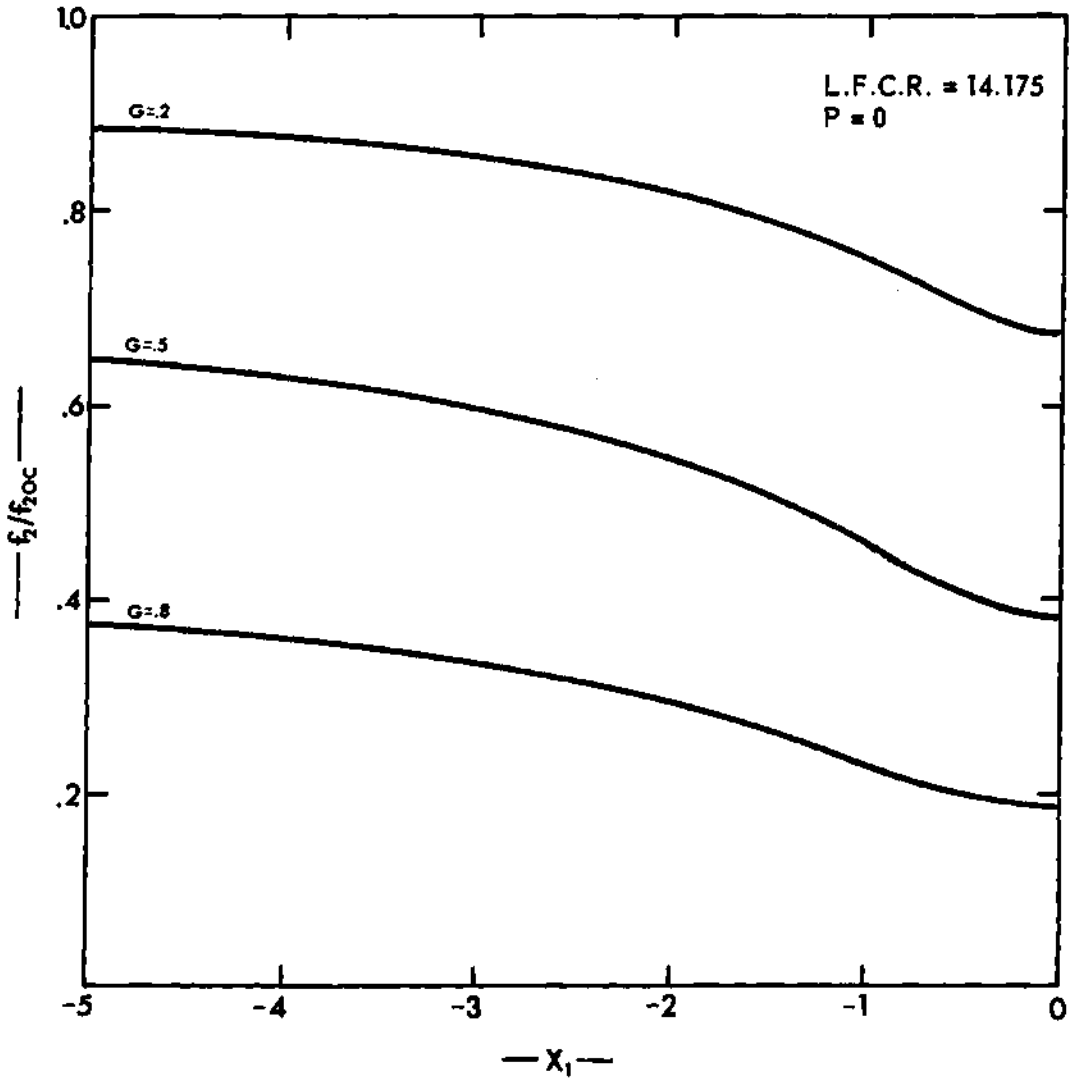

Figure 40. Shift in f_2/f_{2oc} for Constant Loads as x_1 Is Varied for Resembling Hyperbolic Lines, L.F.C.R. = 14.175

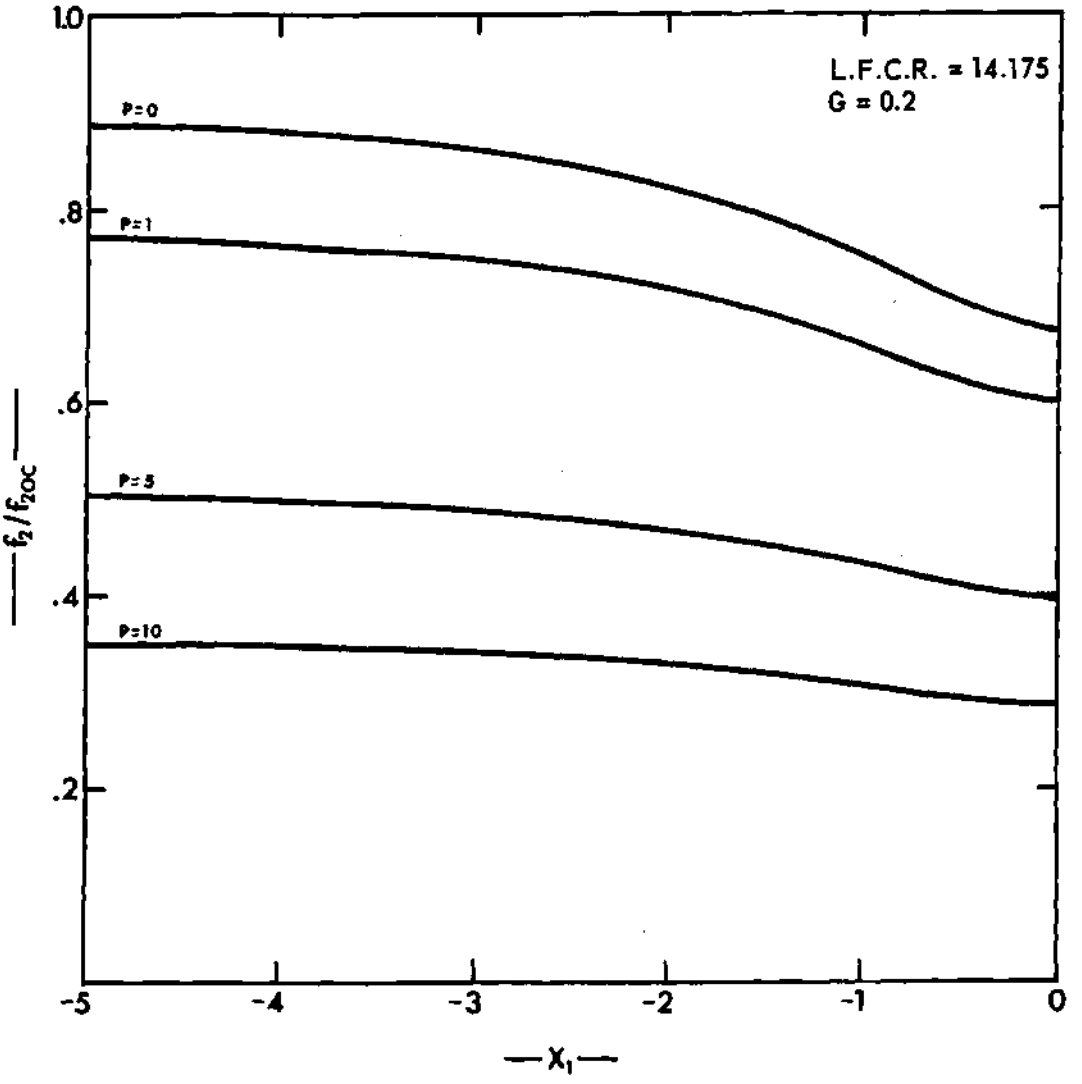

Figure 41. Shift in f_2/f_{2oc} for Constant Loads as x_1 Is Varied for Resembling Hyperbolic Lines, L.F.C.R. = 14.175

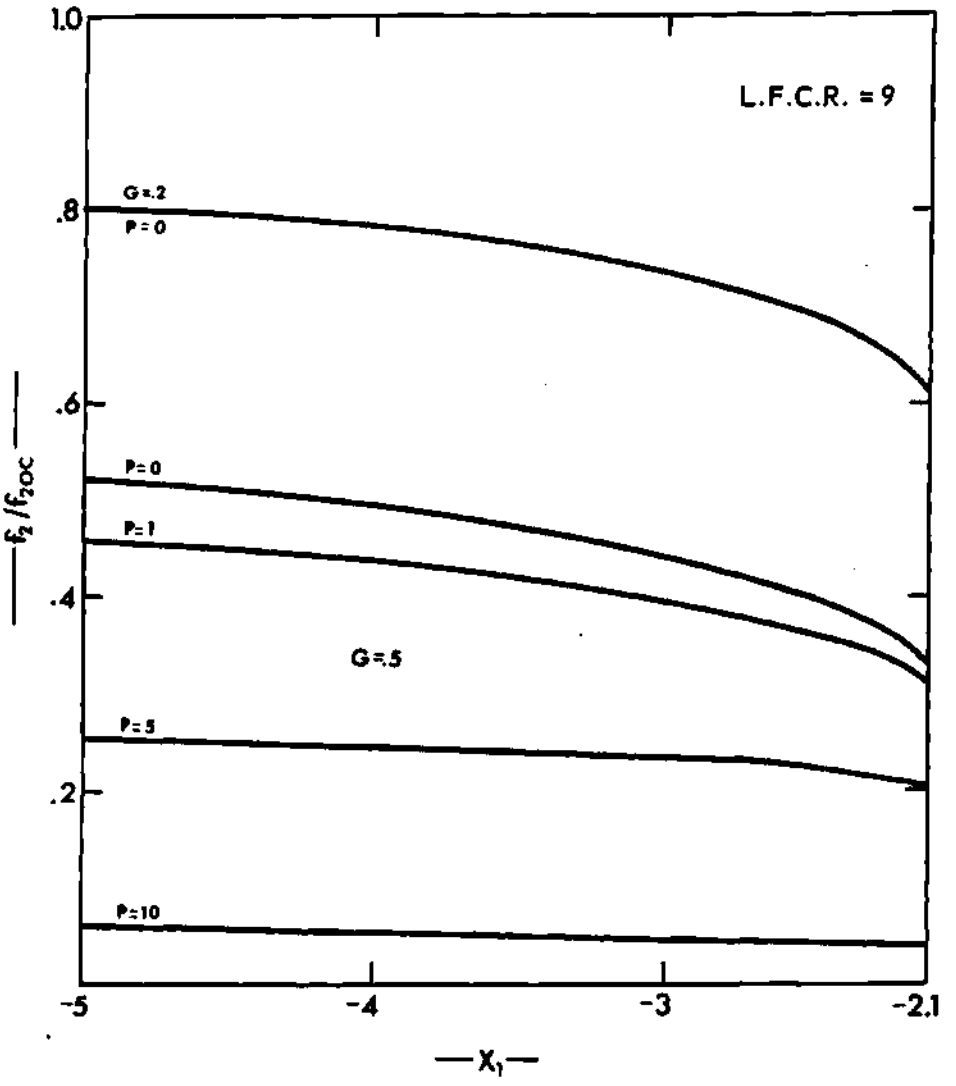

Figure 42. Shift in f_2/f_{2oc} for Constant Loads as x_1 Is Varied for Resembling Hyperbolic Lines, L.F.C.R. = 9

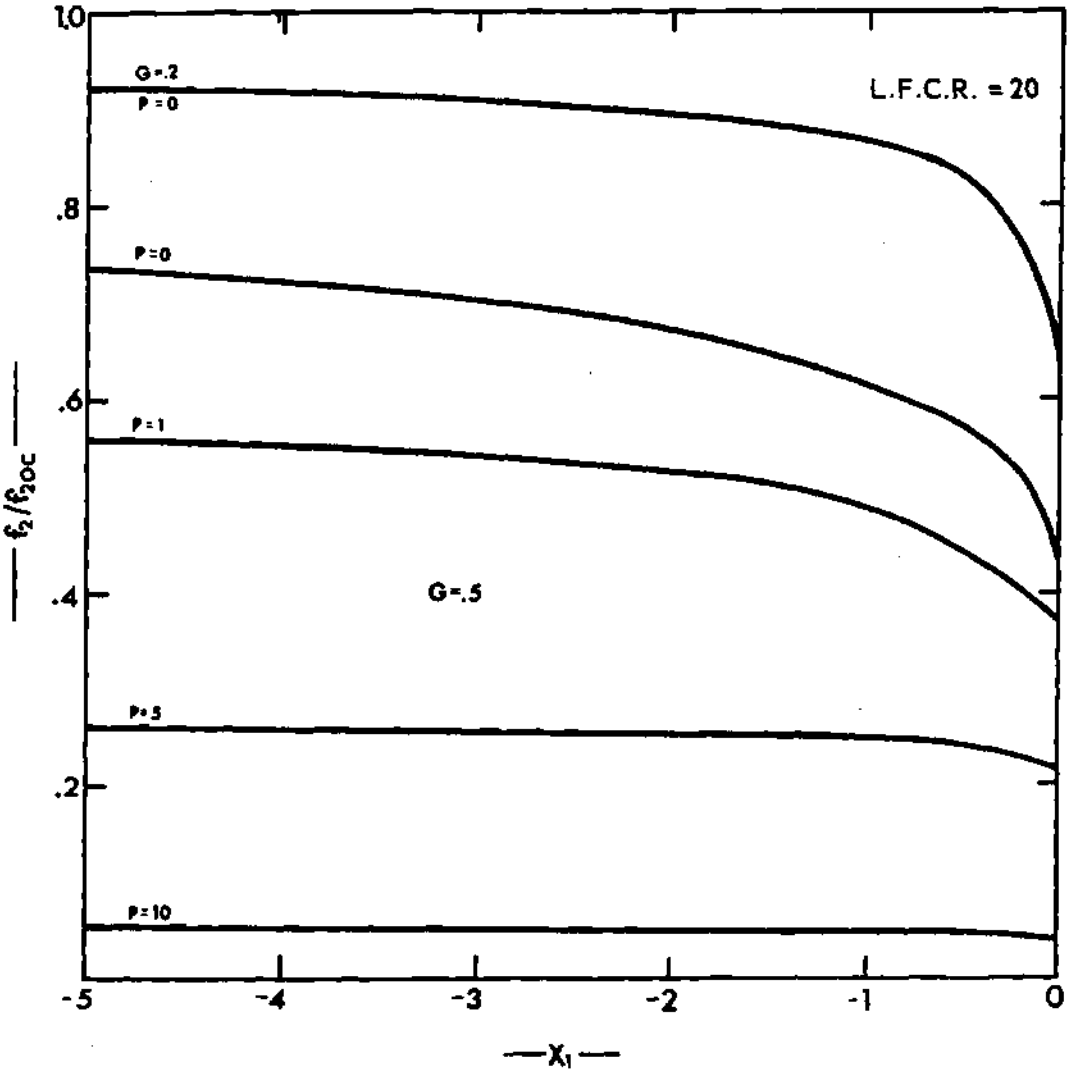

Figure 43. Shift in f_2/f_{2oc} for Constant Loads as x_1 Is Varied for Resembling Hyperbolic Lines, L.F.C.R. = 20

and the contours of Figure 11, the following conclusion concerning the effects of parameter changes on the terminated performance of hyperbolic lines are established: the voltage-transfer characteristics of resembling hyperbolic lines are less susceptible to changes resulting from parallel resistance-capacitance terminations when the value of x_1 is made larger, in the negative direction, or correspondingly when the value of x_2 is made larger.

The results of the above investigations of resembling trigonometric and hyperbolic lines are used to expand previous comparisons of the terminated characteristics of networks from the four general types to include all trigonometric and all hyperbolic lines with low-frequency-cut-off ratios of 9, 14.175, and 20. These comparisons provide a basis for several important theoretical conclusions.

For example, when the theoretical results for those networks with cut-off ratios of 14.175 are compared, it becomes obvious that the voltage-transfer characteristics of the hyperbolic lines with large values of x_1 are less subject to changes in shape due to increased loading. It is also noted that the corresponding performance of trigonometric lines with small values of x_1 is quite different. It is possible to determine the general shape of these networks by examining the location of such trigonometric and hyperbolic networks within their descriptive coordinate systems as depicted in Figure 5. The location of the input and output ports on these illustrations is determined from the above specifications and the contours of Figure 10 and 11. It is obvious that the vast differences in these terminated characteristics are results of their widely different shapes. However, the terminated characteristics of trigonometric lines with large values of x_1, the uniform line and hyperbolic

lines with small negative values of x_1 were essentially identical. The reasons for the similarity is apparent if the values of x_1 and x_2 for the trigonometric and hyperbolic lines are observed. Since in both cases the value of x_1 is almost identical with the value of x_2, there is little variation in the width of either of these networks. Therefore, they are essentially uniform lines and thus should exhibit similar characteristics.

Comparisons of the characteristics of all resembling networks with cut-off ratios of 9 lead to similar conclusions. Here again, the voltage-transfer characteristics of hyperbolic lines with large negative values of x_1 are less subject to changes due to load. However, the terminated characteristics of hyperbolic lines with small negative values of x_1 are very similar to those of the exponential line and trigonometric lines with large values of x_1. Since the values of x_2 for these hyperbolic lines are essentially zero, and since the input ports of these trigonometric lines are located at a value of x that is greater than $\pi/2$, both of these networks had shapes that are similar to that of the exponential line. These shapes can be observed by examining the illustrations of Figure 5 and noting the location of input and output ports.

When the characteristics of the three types of resembling lines with cut-off ratios of 20 are compared, it is observed that their terminated characteristics are similar when x_1 for the hyperbolic line is very small, and x_2 for the trigonometric line approaches zero. Since $\alpha\lambda$ is negative for exponential lines with cut-off ratios greater than 14.175, the width of these lines increases rather than decreases. An examination of Figure 5 shows that the choice of x_1 and x_2 for the hyperbolic and trigonometric lines described above results in networks with similar

tapers. As the value of x_1 for the hyperbolic line is increased, its characteristics are less and less subject to load changes.

Since hyperbolic lines with large negative values of x_1 have the largest values of x_2, the above comparisons illustrate again that distributed networks that have relatively low incremental impedances at their output ports have terminated-voltage-transfer characteristics that are more like those for open-circuit conditions. Correspondingly the transfer characteristics of networks that have relatively large incremental output impedances, such as those for trigonometric lines, are very susceptible to load changes.

When all of the results, comparisons, and conclusions that have been presented in this chapter are reviewed, it is obvious that theoretical verification of the predictions of Chapter 1 has been established. Corresponding experimental verification of these results is presented in the following chapter.

CHAPTER IV

EXPERIMENTAL RESULTS

The results and conclusions presented in Chapter 3 were obtained by applying certain established solutions of equation 1 to standard equations from classical circuit theory. Since the analysis followed reliable mathematical methods, there is no reason to question the validity of any of the theoretical data. However, experimental verification of these results and conclusions produces convincing evidence of both their authenticity and practicability. Since it would obviously be impractical to reconstruct the entire theoretical investigation in a laboratory, this experimental verification is based on the study of characteristics of several representative networks. The trigonometric, uniform, and hyperbolic networks that were used for the initial theoretical comparisons were selected for this investigation.

In actual practice, these networks are constructed in miniature form by depositing thin films of conductive, dielectric and resistive materials on supporting substrates. However, to provide for simplified construction, the networks which were used in this investigation were built on an expanded scale. Such a change in size had no effect on the normalized voltage-transfer characteristics of the networks since their actual shapes were unchanged.

These experimental networks were constructed by sandwiching together in a small press, layers of resistance paper (Teledeltos), Mylar

film, and sheet aluminum. Contacts were made to the Teledeltos by using a silver conductive paint. It was only necessary to shape this layer of resistance paper to produce the desired resistance and capacitance variations. The total values of resistance and capacitance were determined by the resistive coefficient of the Teledeltos and the thickness of the Mylar film.

The solutions of equation 1 for the open circuit impedance parameters on pages 10 and 11 were made under the assumption of one-dimensional current flow. Since the resistance paper used in construction was not an anisotropic material, the prescribed shape of the networks had to be modified to approximate the terminal behavior of a one-dimensional tapered structure. The modification described by Oehler (9) was used to shape the hyperbolic line. Since the width of the uniform line was constant, modification was not required to obtain one-dimensional current flow. Oehler's method was not applicable to modification of trigonometric lines. Therefore, the trigonometric line used in this investigation was simply shaped so that its width varied in proportion to the prescribed capacitance variation.

The hyperbolic line which was first selected for this investigation had its input port located at $x = -5$. Since the hyperbolic cosine of -5 is in excess of 70, the width of this network at its input port was required to be approximately 5000 times its width at $x = 0$. It was obvious that construction of such a network by the method just described would be impracticable. Therefore, a resembling hyperbolic line with $x_1 = -2.5$ and $x_2 = 1.43951$ was used in the experimental investigation.

After the three selected networks were constructed, their open-

circuit-voltage-transfer characteristics were determined experimentally. Although the exact theoretical low-frequency-cut-off ratio of 14.175 was not attained for any of the experimental networks, their normalized open-circuit performance was essentially identical. The normalized-open-circuit-voltage-transfer characteristics for the three networks are depicted in Figure 44 along with the corresponding characteristics which resulted from terminations in simple resistance loads (G = 0.5). The actual values of these resistance loads were determined by doubling the value of load resistance for each network which was required to produce a 30-db-dc attenuation. The marked similarity between the curves of Figure 44 and the corresponding curves of Figures 14 and 17 should be noted.

By terminating each network in certain discrete values of normalized conductance and determining the 30 db attenuation frequency corresponding to each load, data for curves similar to those of Figure 18 were obtained. The theoretical curves of this figure for the uniform and trigonometric lines and a similar theoretical curve for the hyperbolic line used in the experimental investigations are displayed in Figure 45. The corresponding experimental data points for each line are indicated on this figure to provide for comparison of theoretical and experimental results.

In a like manner, Figure 46 depicts both the theoretical and experimental performance of the three networks terminated in certain parallel resistance-capacitance loads. As in Figure 21, these curves illustrate the shift in the curves of Figure 45 as the normalized load capacitance is varied through all practical values.

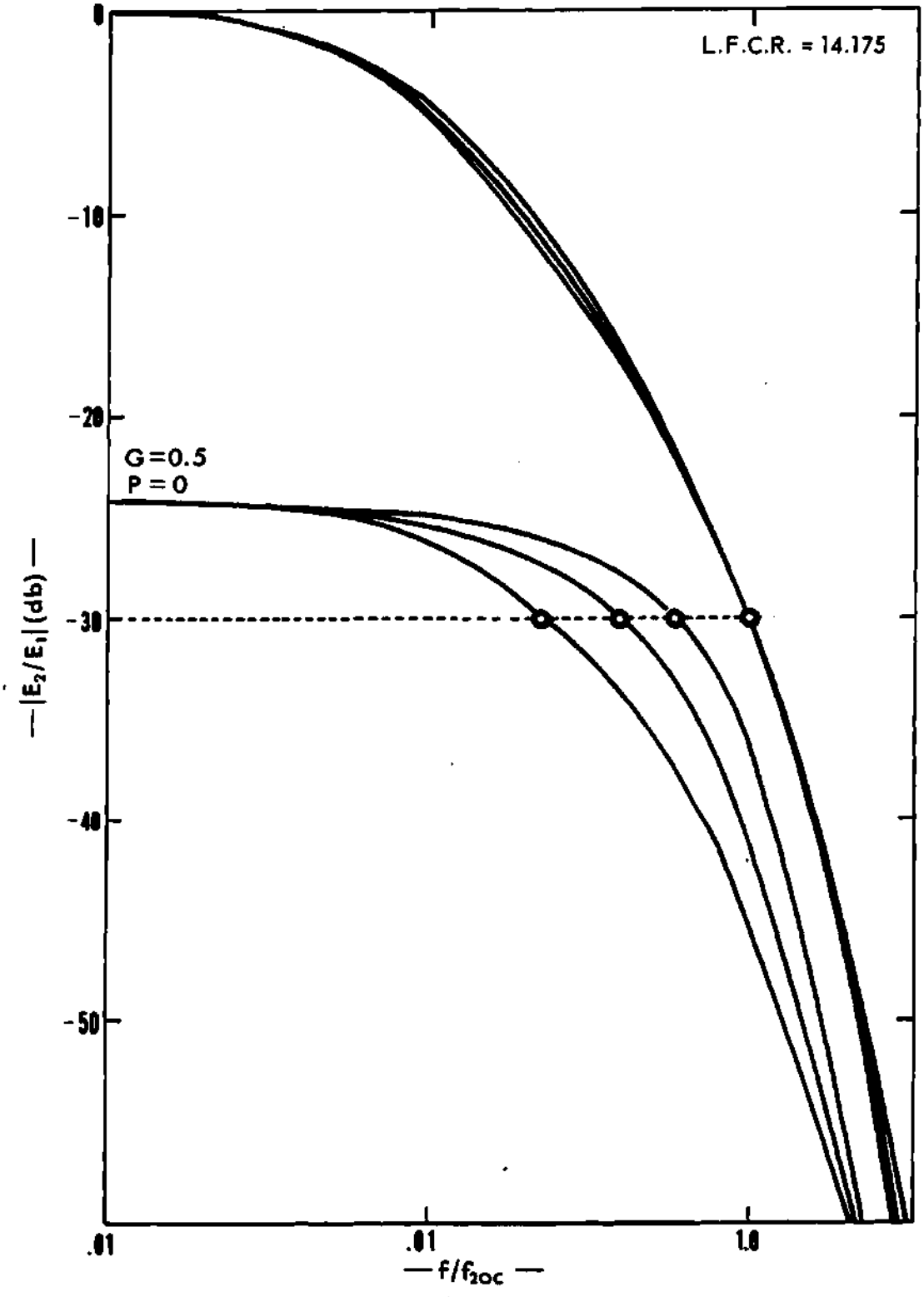

Figure 44. Normalized Experimental Voltage Transfer Characteristics of Three Resembling Lines

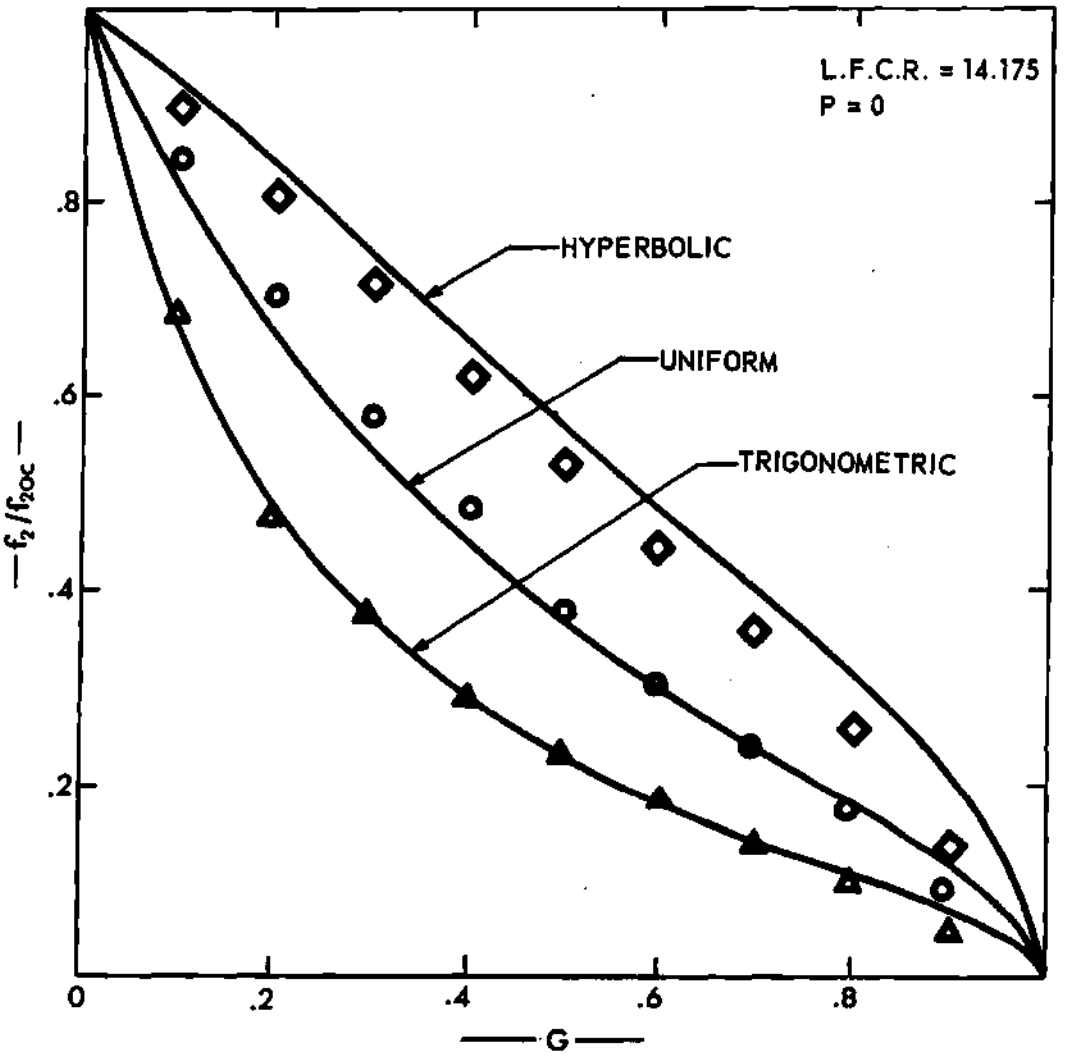

Figure 45. Shift in f_2/f_{2oc} Resulting From Loads with Constant P(P=0) and Variable G for 3 Resembling Lines, L.F.C.R. = 14.175

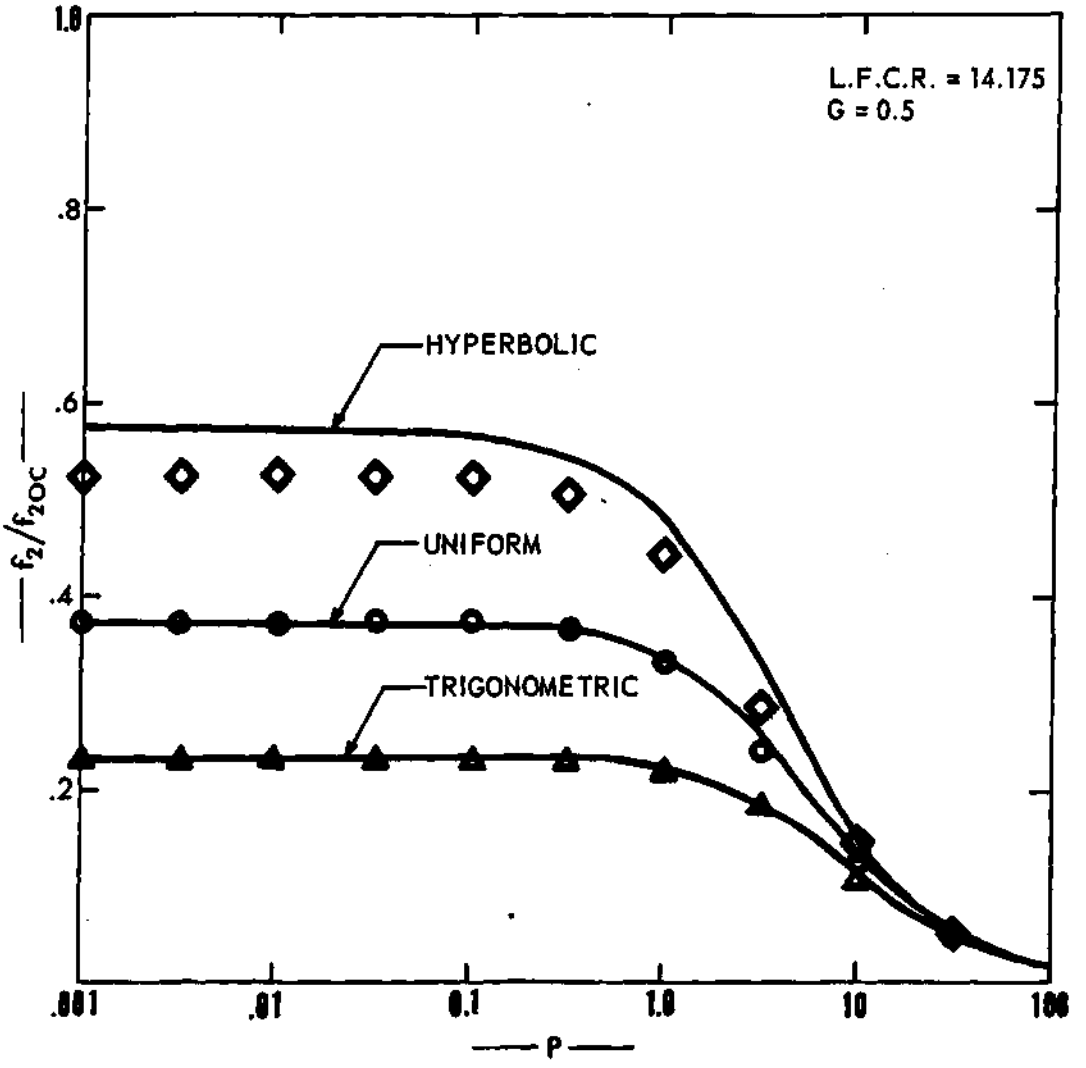

Figure 46. Shift in f_2/f_{2oc} Resulting From Loads with Constant G and Variable P for 3 Resembling Lines, L.F.C.R. = 14.175

The marked similarity between the theoretical and experimental results displayed in Figures 44 and 45 provided convincing evidence of the feasibility of the conclusions made in Chapter 3. The advantages of using distributed networks with relatively low impedances at their output ports are emphasized throughout these conclusions. Therefore, whenever possible RC-thin-film distributed networks which are used in conjunction with finite parallel resistance-capacitance loads should be shaped in the general form of Figure 3D.

BIBLIOGRAPHY

1. J. W. Arnold and P.F. Bechberger, "Sinusoidal Currents in Linearly Tapered Loaded Transmission Lines," Proceedings of the Institute of Radio Engineers, vol. 19, pp. 304-310, February, 1931.

2. C. R. Burrows, "The Exponential Transmission Line," Bell System Technical Journal, vol. 17, pp. 555-573, October, 1938.

3. P. S. Castro and W. W. Happ, "Distributed Parameter Circuits and Microsystem Electronics," Proceedings of the National Electronics Conference, vol. 16, pp. 448-460, 1960.

4. Robert C. Fisher and Allen P. Ziebur, Calculus and Analytic Geometry, Prentice Hall, Englewood Cliffs, New Jersey, 1963, pp. 155-158.

5. C. K. Hager, "Network Design of Microcircuits," Electronics, vol. 32, pp. 44-49, Sept. 1959.

6. I. Jacob, "A Generalization of the Exponential Transmission Lines," Proc. I.R.E., vol. 47, pp. 97-98, Jan. 1959.

7. H. Kaufman, "Bibliography for Nonuniform Transmission Lines," I.R.E. Trans. on Antennas and Propagation, vol. AP-5, pp. 218-220, October 1955.

8. W. M. Kaufman, "Theory of a Monolithic Null Device and Some Novel Circuits," Proc. I.R.E., vol. 48, pp. 1540-1545, Sept. 1960.

9. W. M. Kaufman and S. J. Garrett, "Tapered Distributed Filters," I.R.E. Trans. on Circuit Theory, vol. CT-9, pp. 329-335, Dec. 1962.

10. K. L. Oehler, "A Graphical Design for Exponentially Tapered RC Circuits," IEEE Transactions on Circuit Theory, vol. CT-12, pp. 288-290, June 1965.

11. K. L. Su, "The Trigonometric RC Transmission Lines," IEEE International Convention Record, vol. 11, pt. 2, pp. 43-55, 1963.

12. K. L. Su, "Hyperbolic RC Transmission Line," Electronics Letters, vol. 1, pp. 59-60, May, 1965.

13. K. L. Su, "The Selectivity of Notch Filters Using Nonuniform RC Lines," Electronics Letters, vol. 1, pp. 204-206, Sept. 65.

14. K. L. Su, "The Effect of Load Conductance on the Selectivity of Notch Filters," Electronics Letters, vol. 1, pp. 217-219, October 1965.

15. A. T. Starr, "The Nonuniform Transmission Line," Proc. I.R.E., vol. 20, pp. 1052-1063, June 1932.

16. Iwao Sugai, "A Table of Solutions of Riccati's Equations," Proc. I.R.E., vol. 50, pp. 2124-2126, October 1962.

17. B. L. H. Wilson and R. B. Wilson, "Shaping of Distributed RC Networks," Proc. I.R.E., vol. 49, pp. 1330-1331, August 1961.